

Understanding Nanoparticle Transport in Human Vasculature Through Large-scale Fluid-Structure Interaction Simulations

Ying Li

Assistant Professor

Department of Mechanical Engineering

University of Connecticut

Storrs CT

Email: ying.3.li@uconn.edu

Collaborators: Wing Kam Liu, Northwestern University; Martin Kroger, ETH Zurich; Dean Ho, UCLA; Paolo Decuzzi, Italian Institute of Technology; Mu-Ping Nieh, Jessica Rouge, Mei Wei, Xiuling Lu, UConn; Lucy Zhang, RPI

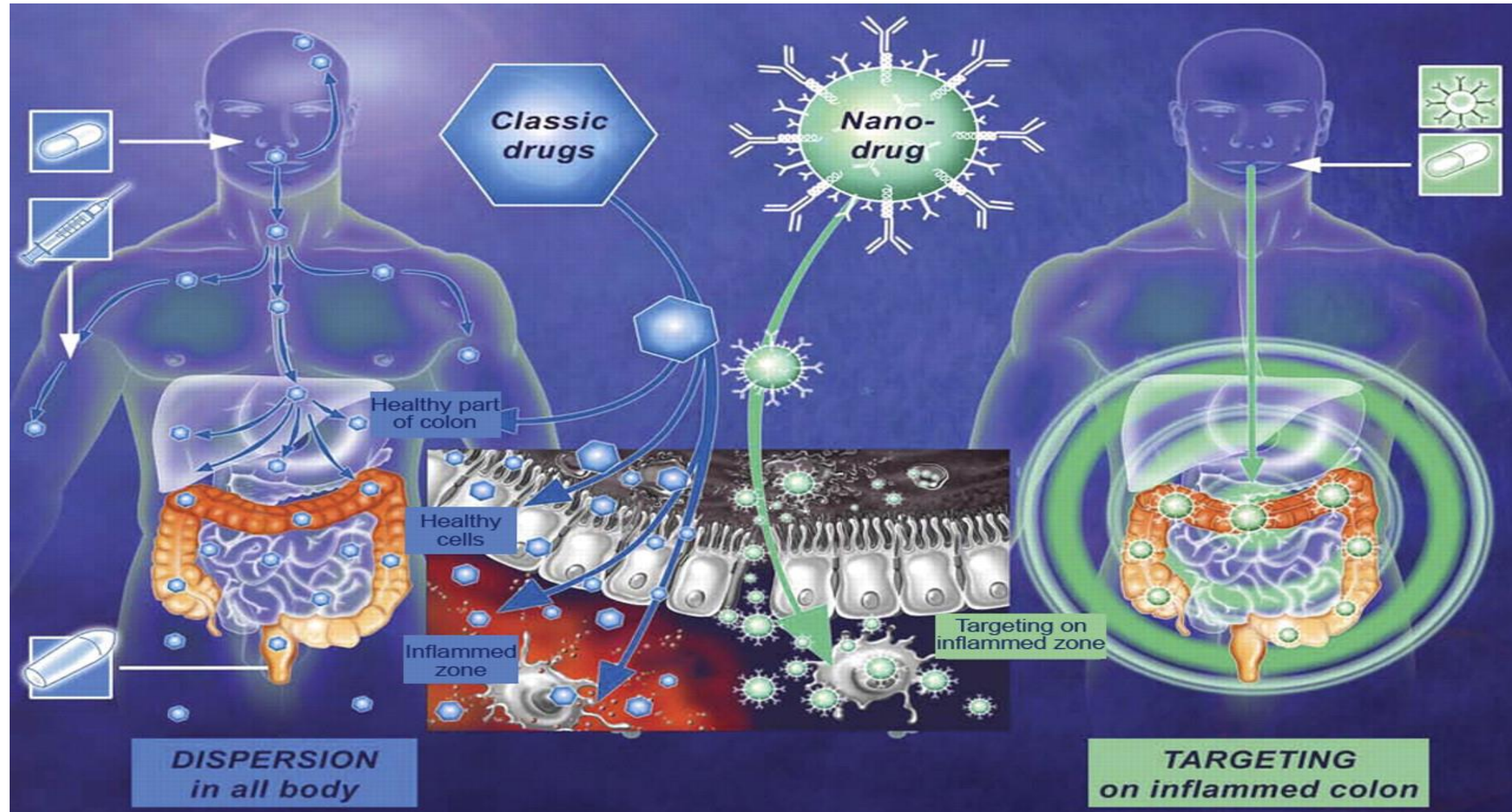
Students: Dr. Huilin Ye (Cadence), Dr. Zhiqiang Shen (ORNL), Alessandro Fisher, William Baker (REU), Jeffrey Ge (REU)

Palabos Online Seminar Series, September 1st, 5:00 pm CET, 2021

- ❑ Background
- ❑ Computational framework
- ❑ Validation and Verification
- ❑ Results
 - Anomalous vascular dynamics of nanoworms within blood Flow
 - Adhesion effect on margination of elastic micro-particles
 - Motion of particle under external magnetic field
- ❑ Conclusion and Ongoing work

Nanomedicine:

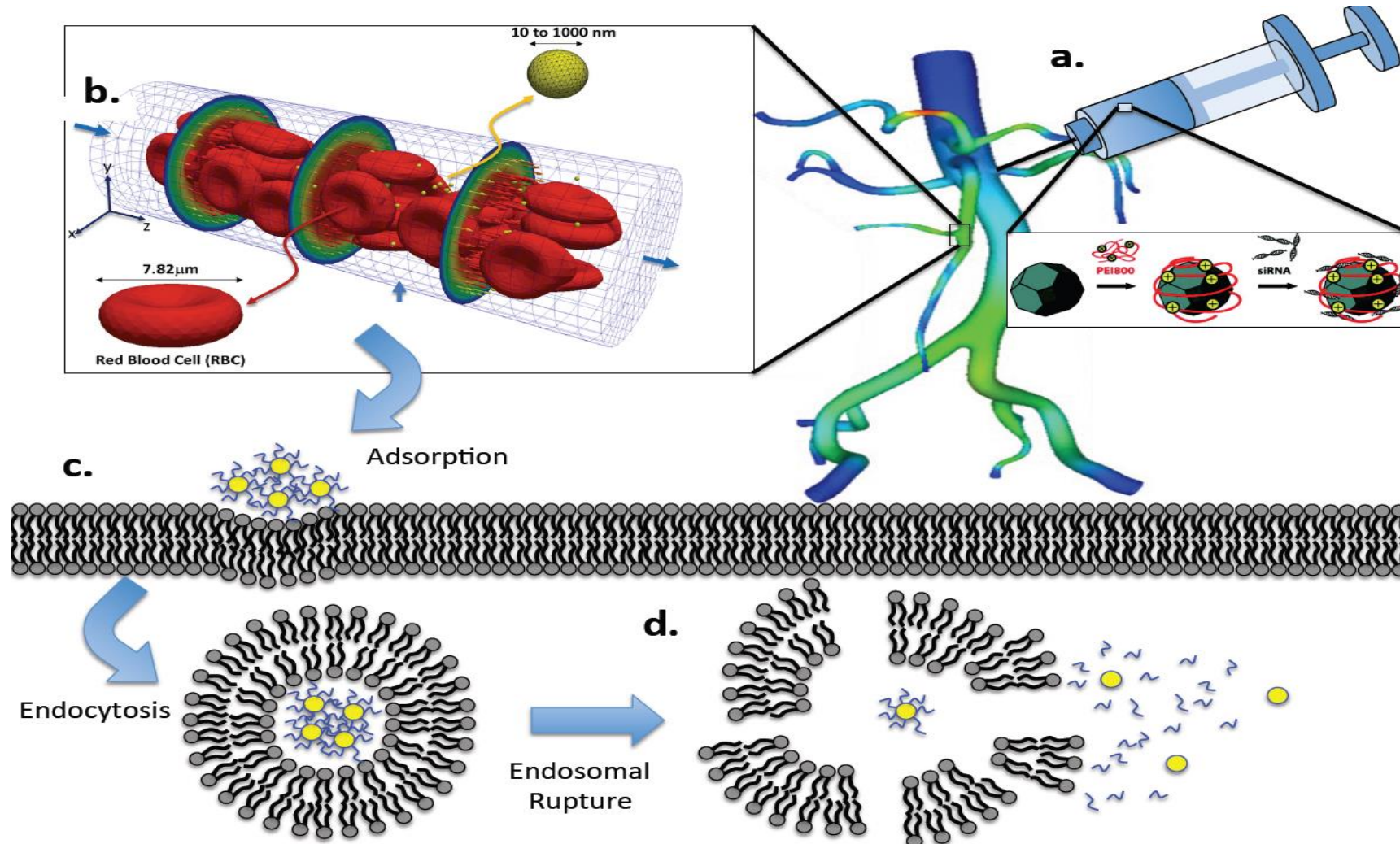
a promising method to deliver drugs to diseased



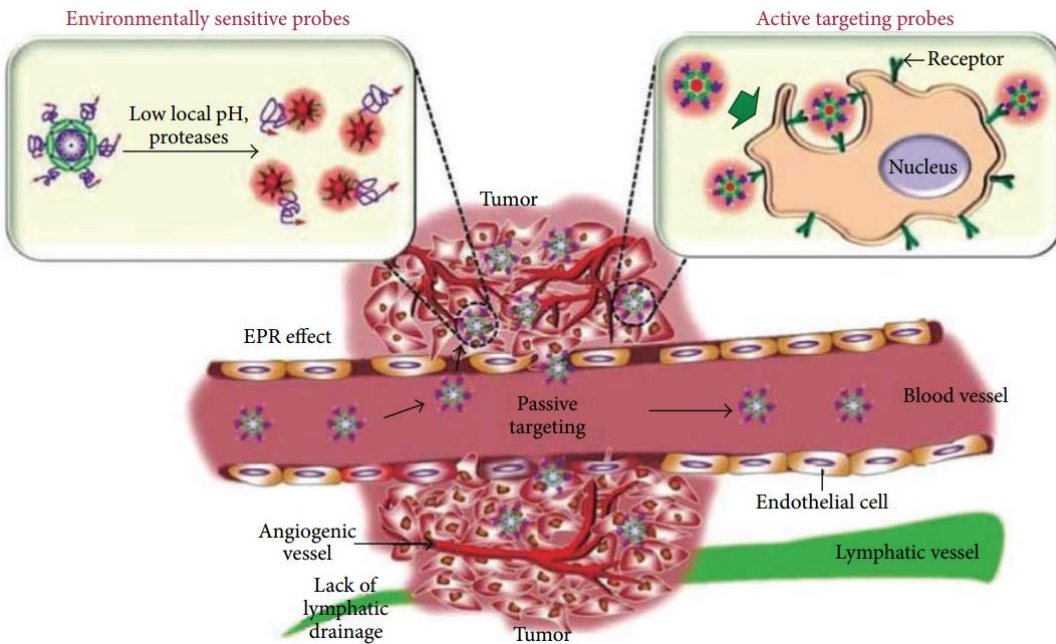


Computational design of efficient drug carriers

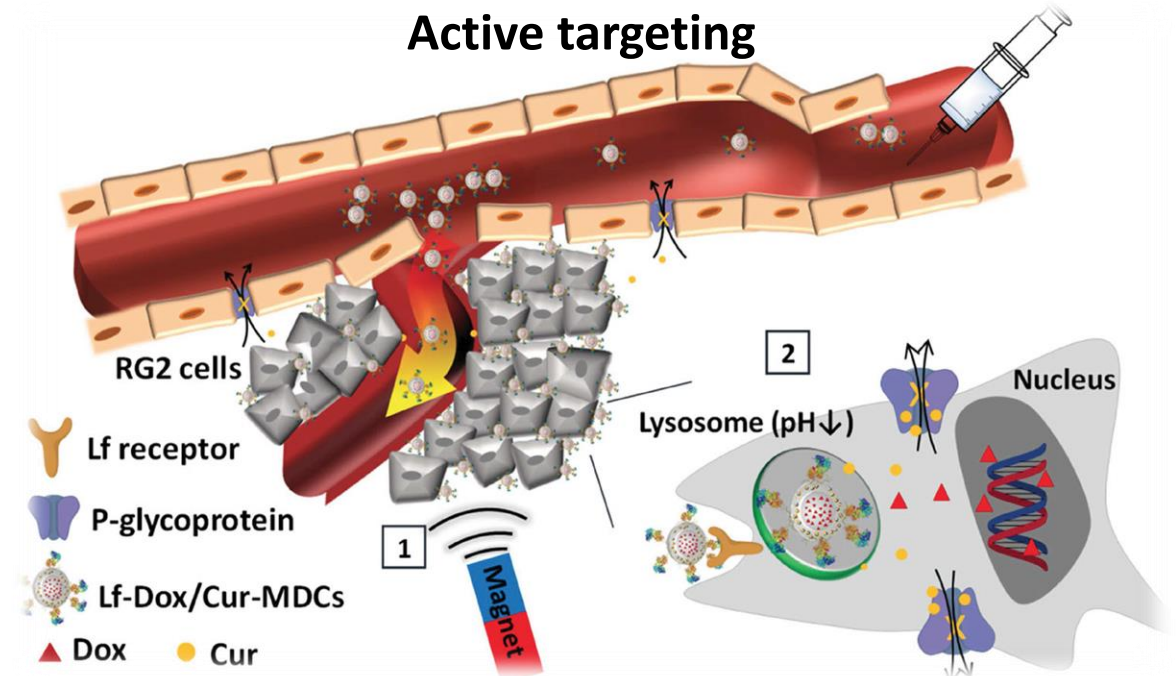
Goal : Design nanoparticle-based drug carriers for efficient and targeted drug delivery via predictive multiscale modeling



Passive targeting



Active targeting



Life journey

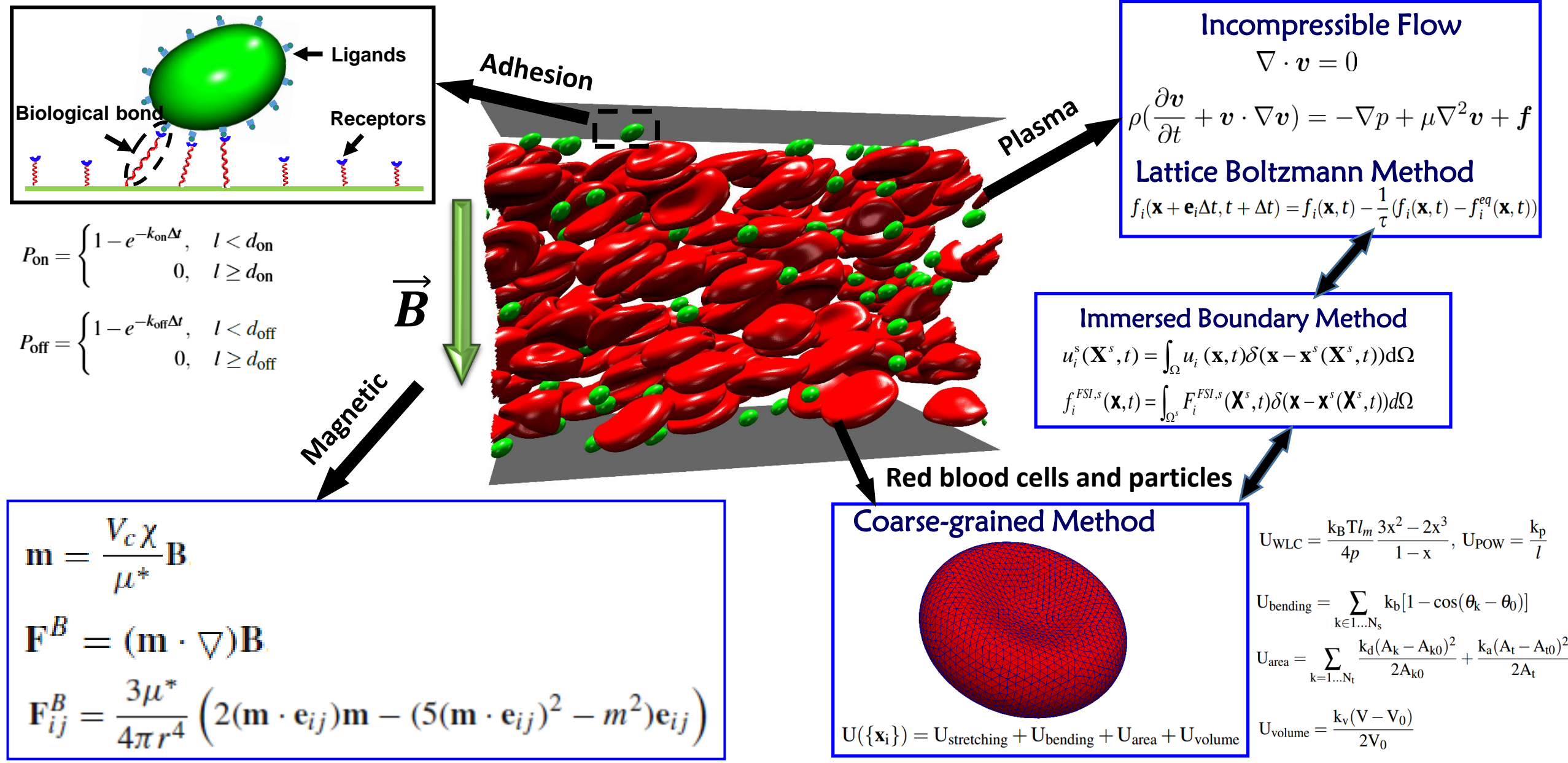
- Transport and circulation with RBCs, WBCs, and others in normal vascular network
- Firm adhesion to the vessel wall near tumor site
- Diffusion into tumor site through 'leaky' vessel walls
- Recognition and uptake by tumor cells

Intrinsic properties

- Size
- Shape
- Stiffness
- Surface functionality

External triggering

- Electrical
- **Magnetical**
- Chemical
- Optical



The lattice-Boltzmann algorithm is a popular method used to simulate the hydrodynamics of complex fluids on a grid. As this method requires only nearest neighbor grid point information, it is very straightforward to implement, and is ideally suited for large-scale parallel applications.

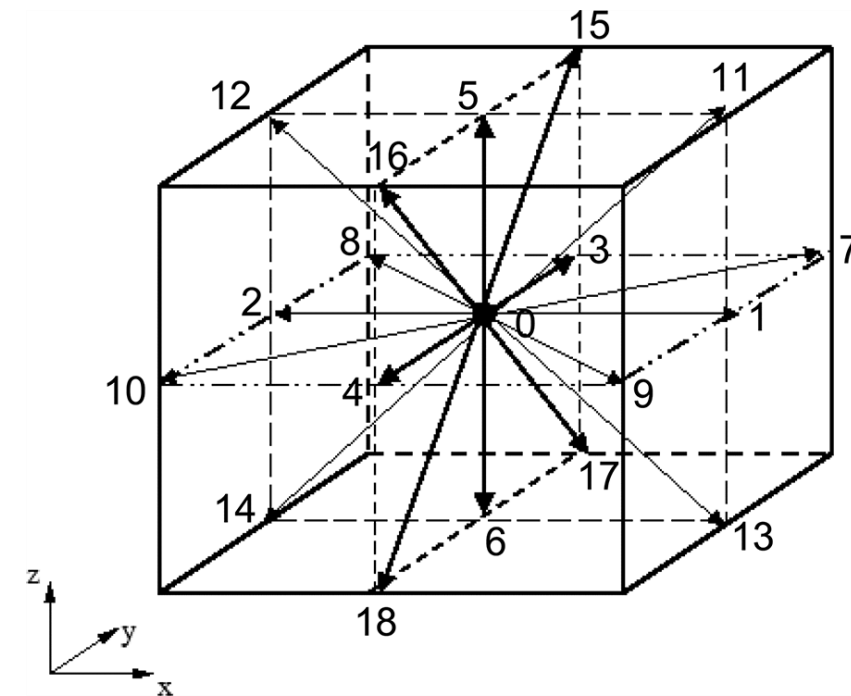
- Navier-Stokes equations with thermal noise (Landau & Lifshitz):

$$(\partial_t + \partial_\alpha u_\alpha) \rho = 0$$

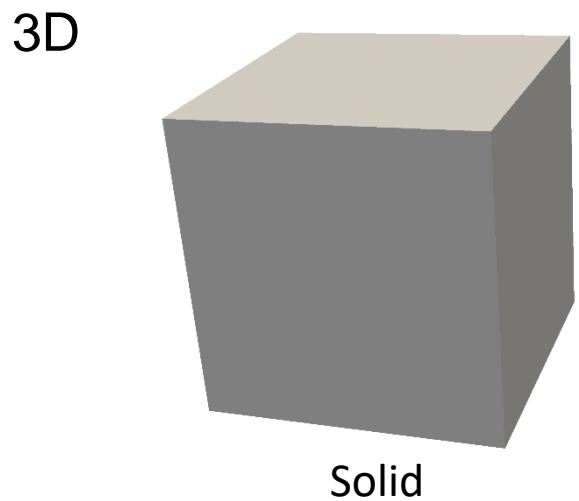
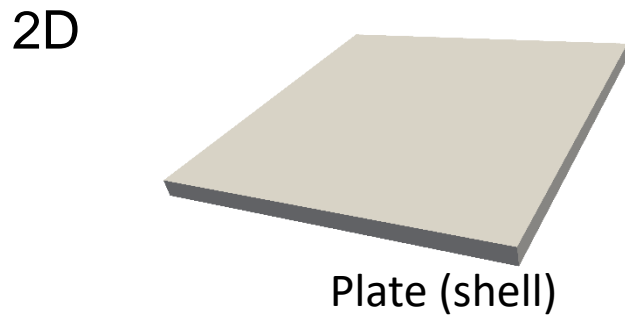
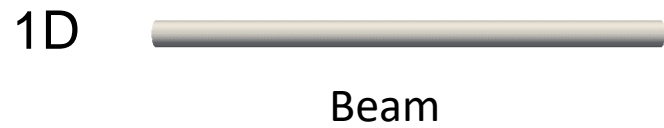
$$\rho(\partial_t + u_\alpha \partial_\alpha) u_\beta = -\partial_\alpha (P_{\beta\alpha} + s_{\beta\alpha}) + \partial_\alpha (\eta_{\alpha\beta\gamma\nu} \partial_\gamma u_\nu) + F_\beta$$

- Note that the thermal noise appears in the stress tensor so will conserve mass and momentum. It should also obey the fluctuation-dissipation theorem (Landau & Lifshitz):

$$\langle s_{\alpha\beta}(\mathbf{r}, t) s_{\gamma\nu}(\mathbf{r}', t') \rangle = 2k_B T \eta_{\alpha\beta\gamma\nu} \delta(\mathbf{r} - \mathbf{r}') \delta(t - t')$$



Structure: Lattice Model

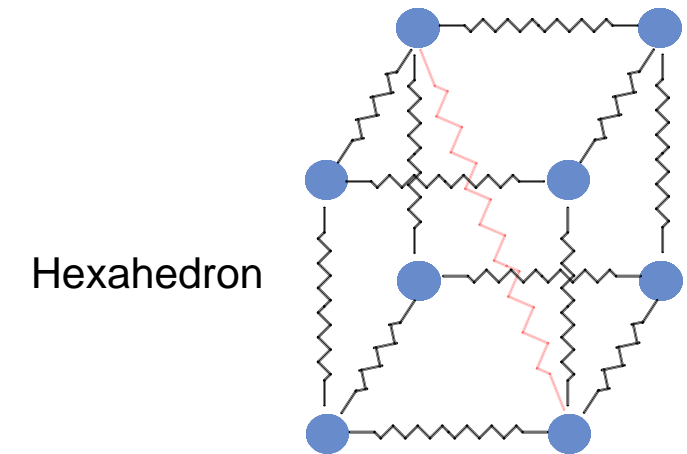
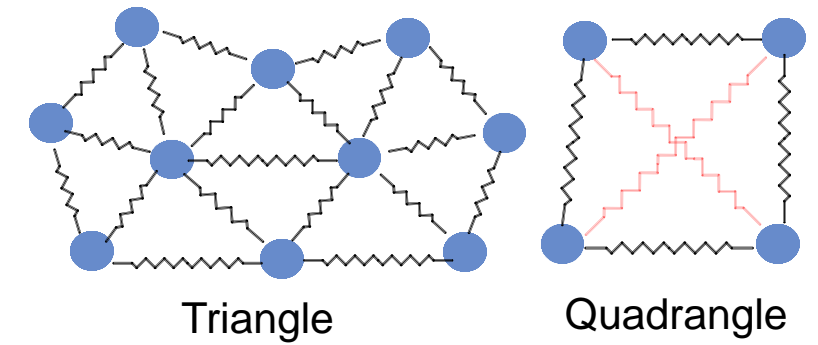
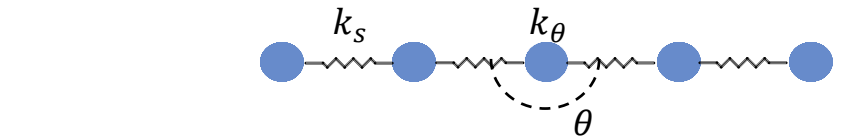


Continuum model

In-plane shear Area compression
Young's modulus Bending stiffness



Spring constant Bending spring
Area constrain Volume constrain



Hexahedron

Lattice model

Shell (Red blood cell and sphere)

$$U(\{\mathbf{x}_i\}) = U_{\text{stretching}} + U_{\text{bending}} + U_{\text{area}} + U_{\text{volume}}$$

In-plane stretching (bond)

$$U_{\text{WLC}} = \frac{k_B T l_m}{4p} \frac{3x^2 - 2x^3}{1-x}, \quad U_{\text{POW}} = \frac{k_p}{l}$$

Out-plane bending (dihedral)

$$U_{\text{bending}} = \sum_{k \in 1 \dots N_s} k_b [1 - \cos(\theta_k - \theta_0)]$$

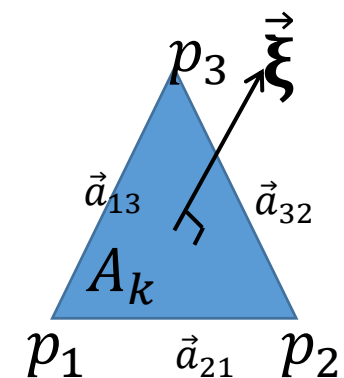
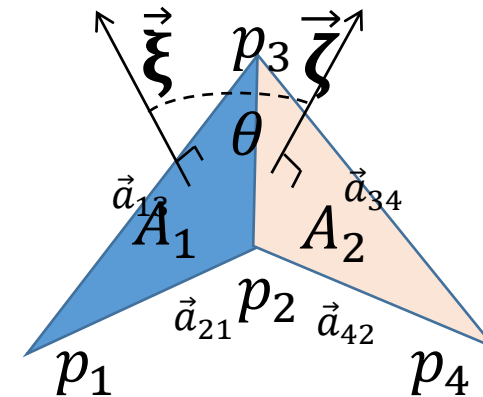
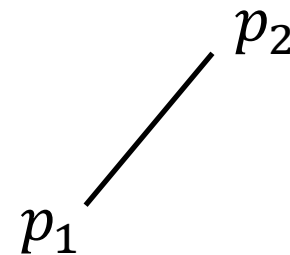
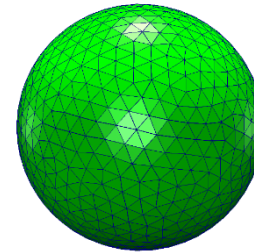
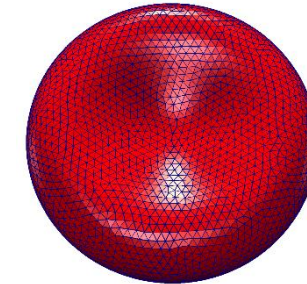
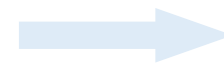
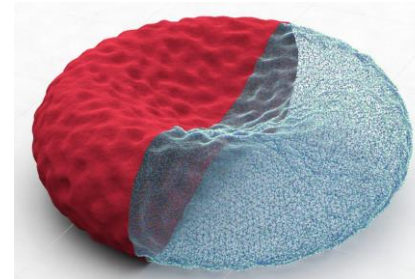
Area incompressibility of the lipid bilayer

$$U_{\text{area}} = \sum_{k=1 \dots N_t} \frac{k_d (A_k - A_{k0})^2}{2A_{k0}} + \frac{k_a (A_t - A_{t0})^2}{2A_t}$$

Incompressibility of the inner cytosol

$$U_{\text{volume}} = \frac{k_v (V - V_0)}{2V_0}$$

Lattice model



Shear modulus

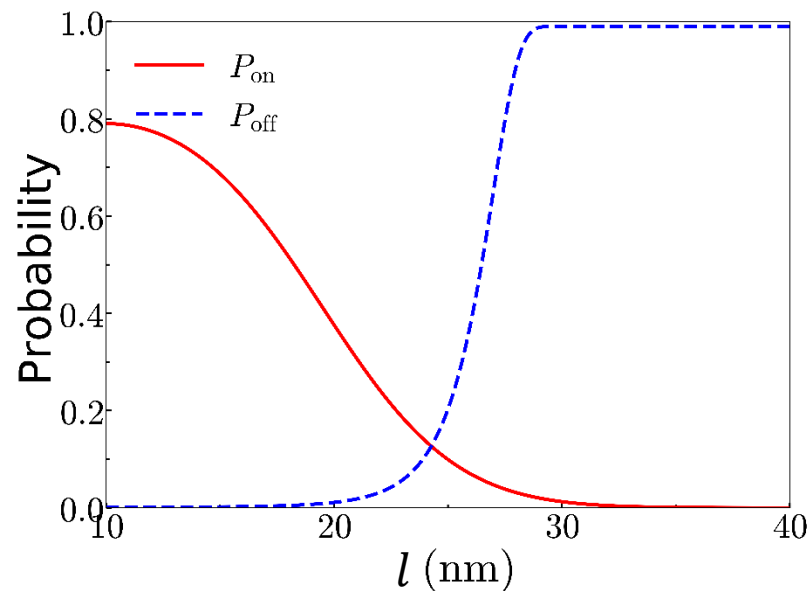
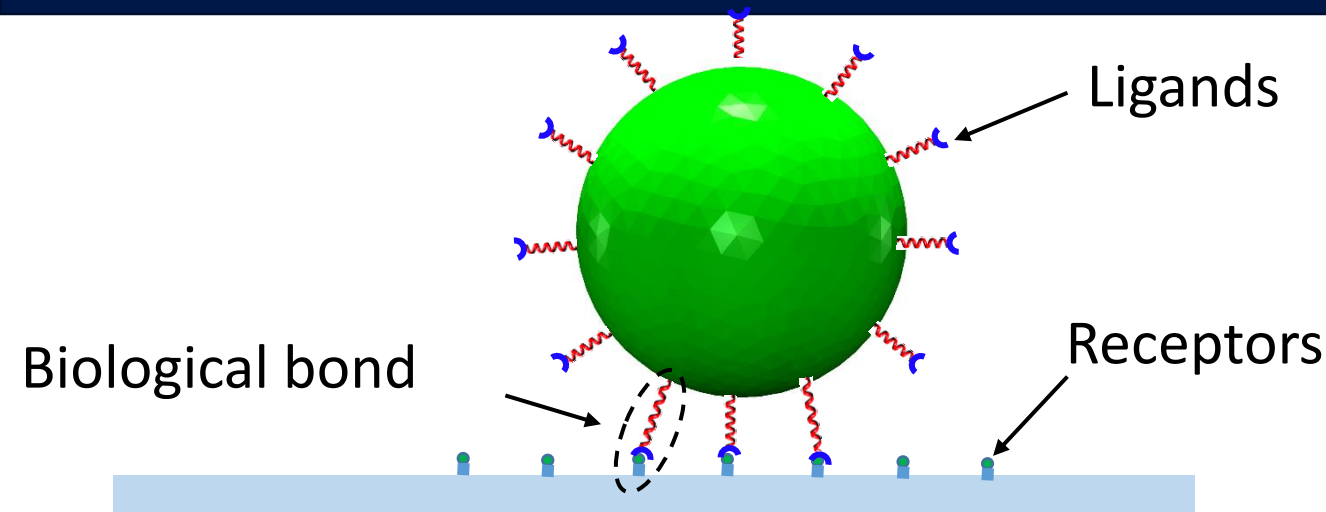
$$\mu_0 = \frac{\sqrt{3} k_B T}{4 p l_m x_0} \left(\frac{x_0}{2(1-x_0)^3} - \frac{1}{4(1-x_0)^2} + \frac{1}{4} \right) + \frac{3\sqrt{3} k_p}{4 l_0^3}$$

Area compression modulus

$$K = 2\mu_0 + k_a + k_d$$

Young's modulus

$$Y = \frac{4K\mu_0}{K + \mu_0}$$



$$F(l) = k_s(l - l_0)$$

One-to-One interaction!

$$P_{on} = \begin{cases} 1 - e^{-k_{on}\Delta t} & \text{for } l < d_{on} \\ 0 & \text{for } l \geq d_{on} \end{cases}$$

$$P_{off} = \begin{cases} 1 - e^{-k_{off}\Delta t} & \text{for } l < d_{off} \\ 1 & \text{for } l \geq d_{off} \end{cases}$$

$$k_{on} = k_{on}^0 \exp\left(-\frac{\sigma_{on}(l - l_0)^2}{2k_B T}\right)$$

$$k_{off} = k_{off}^0 \exp\left(\frac{\sigma_{off}(l - l_0)^2}{2k_B T}\right)$$

- k_{on} Reaction rate
- k_{off} Dissociation rate
- σ_{on} Effective on strength
- σ_{off} Effective off strength

Immersed boundary method

1. Advance of fluid field

$$f_i(\mathbf{x} + \mathbf{c}_i \Delta t, t + \Delta t) - f_i(\mathbf{x}, t) = -\frac{\Delta t}{\tau} (f_i - f_i^{\text{eq}}) + F_i \Delta t$$

2. Velocity interpolation

$$u_i^s(\mathbf{X}^s, t) = \int_{\Omega} u_i(\mathbf{x}, t) \delta(\mathbf{x} - \mathbf{x}^s(\mathbf{X}^s, t)) d\Omega$$

3. Update solid field

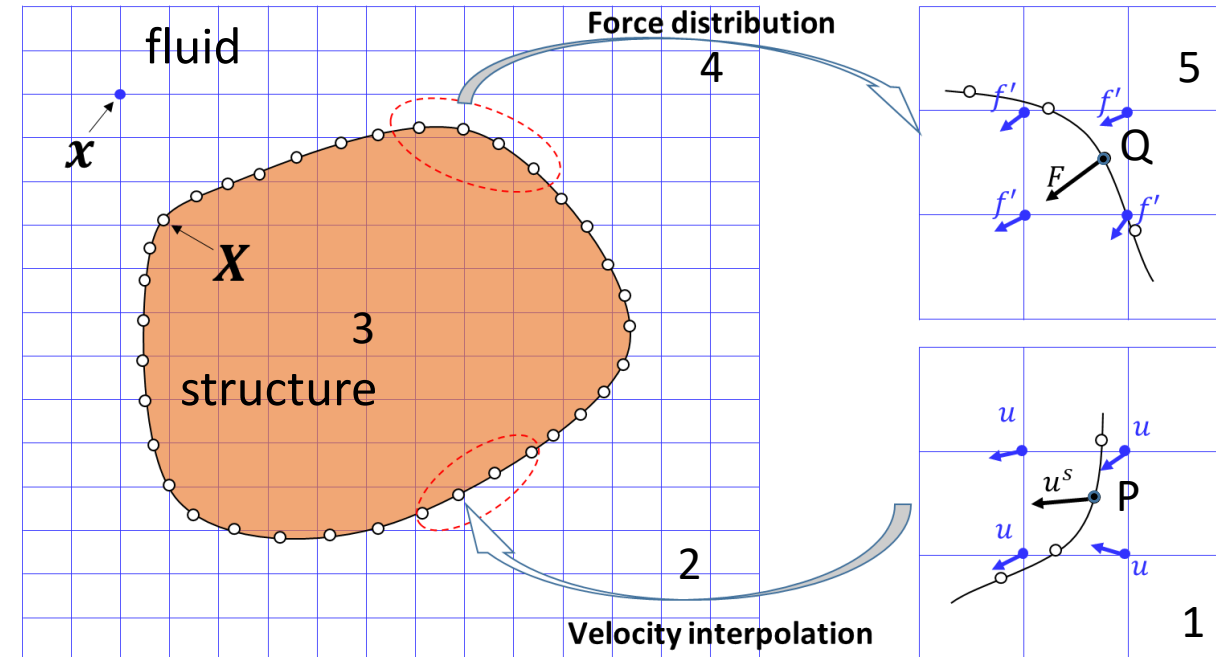
$$U = \mu^s (I_1 - 3)/2 + \lambda (\ln J)^2 / 2 - \mu^s \ln J$$

4. Force distribution

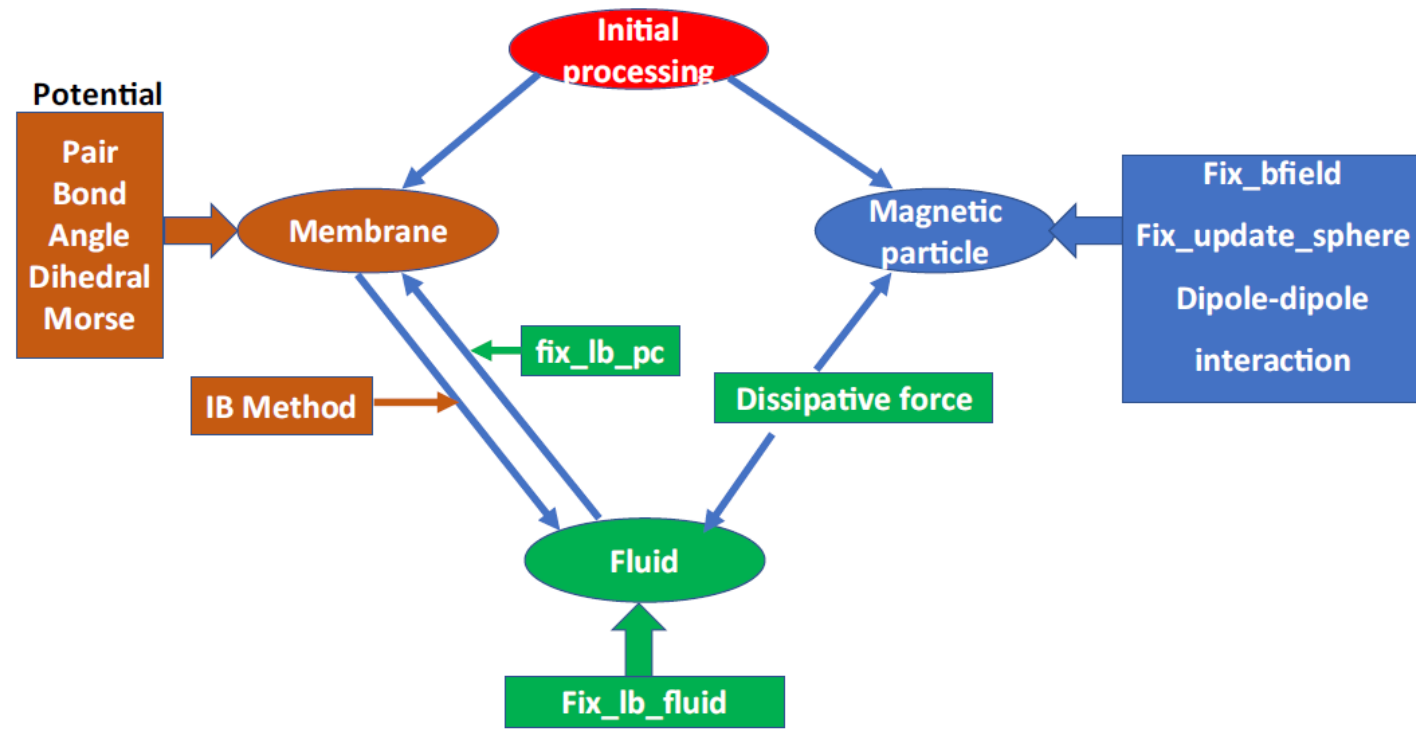
$$f_i^{FSI,s}(\mathbf{x}, t) = \int_{\Omega^s} F_i^{FSI,s}(\mathbf{X}^s, t) \delta(\mathbf{x} - \mathbf{x}^s(\mathbf{X}^s, t)) d\Omega$$

5. Advance fluid field with body force

$$f_i(\mathbf{x} + \mathbf{c}_i \Delta t, t + \Delta t) - f_i(\mathbf{x}, t) = -\frac{\Delta t}{\tau} (f_i - f_i^{\text{eq}}) + F_i \Delta t$$



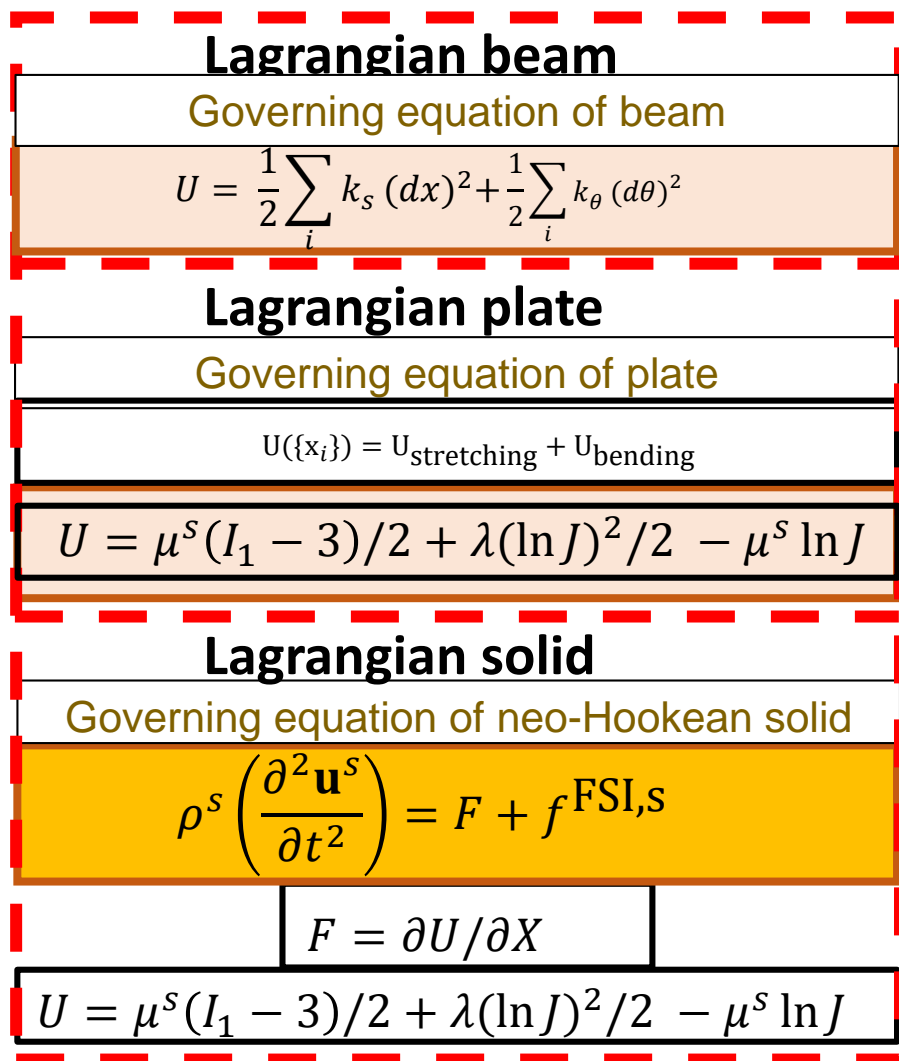
$$\delta(r) = \begin{cases} \frac{1}{4} \left(1 + \cos \left(\frac{\pi |r|}{2} \right) \right), & r \leq 2 \\ 0, & r > 2 \end{cases}$$



Implementation in LAMMPS:

- MPI domain decomposition taken same as particles in LAMMPS
- Implemented as fixes:
 - `fix lb_fluid` – applies force of particle on fluid
 - `fix viscous_lb` – applies force of fluid on particles along with `fix_momentum_lb`
- Hook into `update.cpp` : units
Otherwise just a regular user package

LAMMPS is a classical molecular dynamics code with a focus on materials modeling. It's an acronym for Large-scale Atomic/Molecular Massively Parallel Simulator. LAMMPS has potentials for solid-state materials (metals, semiconductors) and soft matter (biomolecules, polymers) and coarse-grained or mesoscopic systems. It can be used to model atoms or, more generically, as a parallel particle simulator at the atomic, meso, or continuum scale.



LAMMPS

$$u_i^m(\mathbf{X}^m, t) = \int_{\Omega} u_i(\mathbf{x}, t) \delta(\mathbf{x} - \mathbf{x}^m(\mathbf{X}^m, t)) d\Omega$$

$$u_i^s(\mathbf{X}^s, t) = \int_{\Omega} u_i(\mathbf{x}, t) \delta(\mathbf{x} - \mathbf{x}^s(\mathbf{X}^s, t)) d\Omega$$

Velocity interpolation

IBM

Incompressible fluid solver

$$(\partial_t + e_{i\alpha} \partial_\alpha) f_i = -\frac{1}{\tau} (f_i - f_i^{eq}) + f_i^{\text{FSI},m} + f_i^{\text{FSI},s}$$

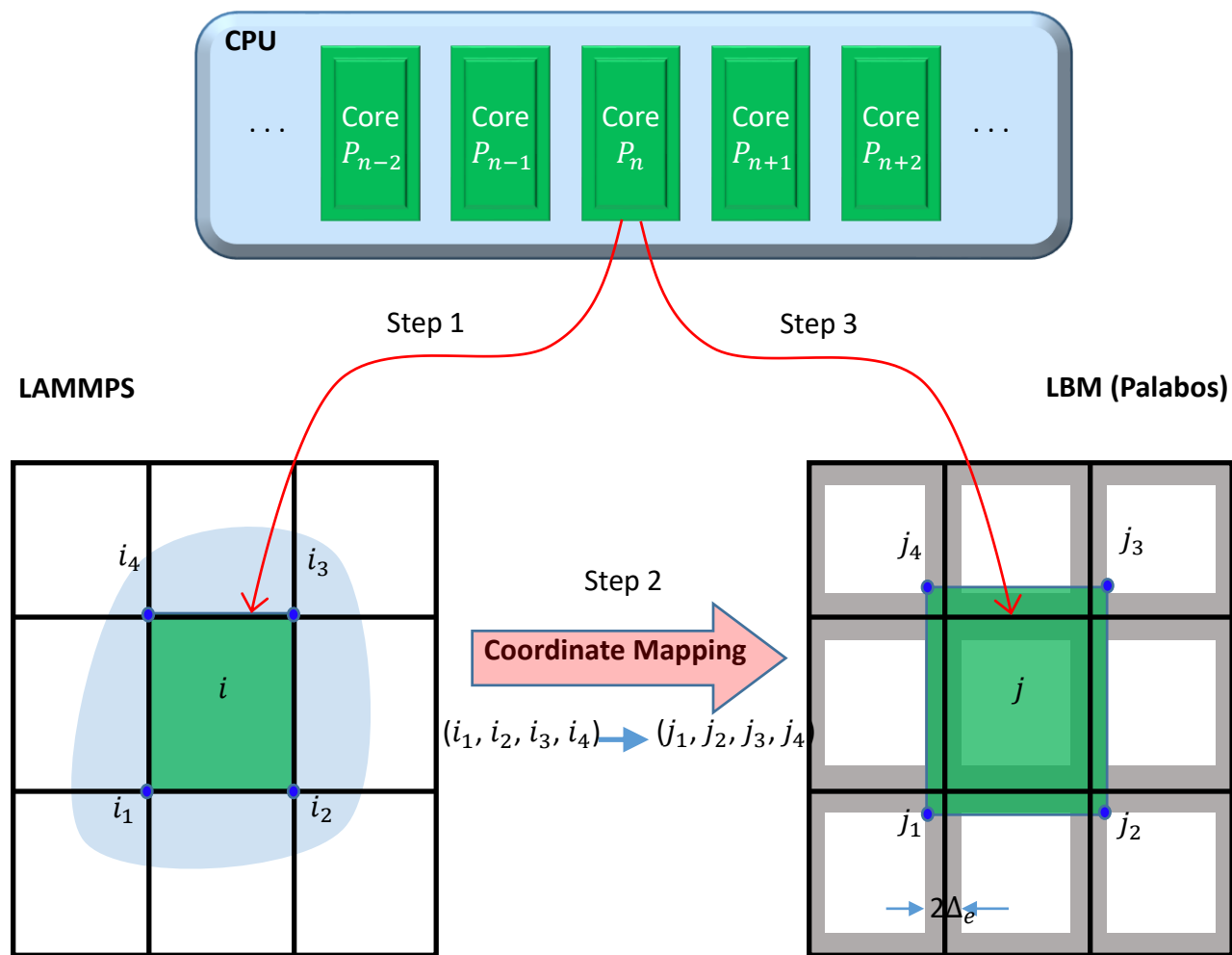
LBM

IBM

Force distribution

$$f_i^{\text{FSI},m}(\mathbf{x}, t) = \int_{\Omega^s} f_i^{\text{FSI},m}(\mathbf{X}^m, t) \delta(\mathbf{x} - \mathbf{x}^m(\mathbf{X}^m, t)) d\Omega$$

$$f_i^{\text{FSI},s}(\mathbf{x}, t) = \int_{\Omega^s} f_i^{\text{FSI},s}(\mathbf{X}^s, t) \delta(\mathbf{x} - \mathbf{x}^s(\mathbf{X}^s, t)) d\Omega$$



CPU mapping to complete velocity interpolation and force spreading

Algorithm 1: Immersed boundary-based spatial decomposition

```

Run LAMMPS
Read simulation box  $\Gamma$ 
Partition  $\Gamma$  into  $N$  regular bricks      #comm_brick
Run interface                               #contained in file: latticeDecomposition.hh
Pass bricks information to Palabos
Run Palabos
Create  $N$  blocks with the information from LAMMPS
For loop  $m$  in  $N$  blocks
    Assign block information to processor numbered  $n$ 
End loop
Initialization parallelism in Palabos
    
```

Algorithm 2: Data communication between LAMMPS and Palabos

```

Run LAMMPS
Obtain coordinates of structure nodes  $\mathbf{x}(\mathbf{X}, t)$ , and pass them to IB interface.
Run Palabos
Obtain the velocity of fluid nodes  $\mathbf{u}(\mathbf{x}, t)$ , and pass them to IB interface.
Run IB interface                               #contained in files: ibm2D.hh or ibm3D.hh
Interpolate the velocity  $\mathbf{u}^s$  at location  $\mathbf{x}(\mathbf{X}, t)$ , and return them to LAMMPS.
Run LAMMPS
Calculate the FSI force  $\mathbf{F}$ , and pass them to IB interface
Run IB interface                               #contained in files: ibm2D.hh or ibm3D.hh
Spread FSI force  $\mathbf{F}$  to the fluid nodes  $\mathbf{f}'$  at location  $(\mathbf{x}, t)$ , and pass them to Palabos.
Run Palabos
Use the body force nodes  $\mathbf{f}'$  to advance fluid field.
Run LAMMPS
Use FSI force  $\mathbf{F}$  to update the new location of structure.
    
```

Stretching of a single RBC

(a)

Original shape



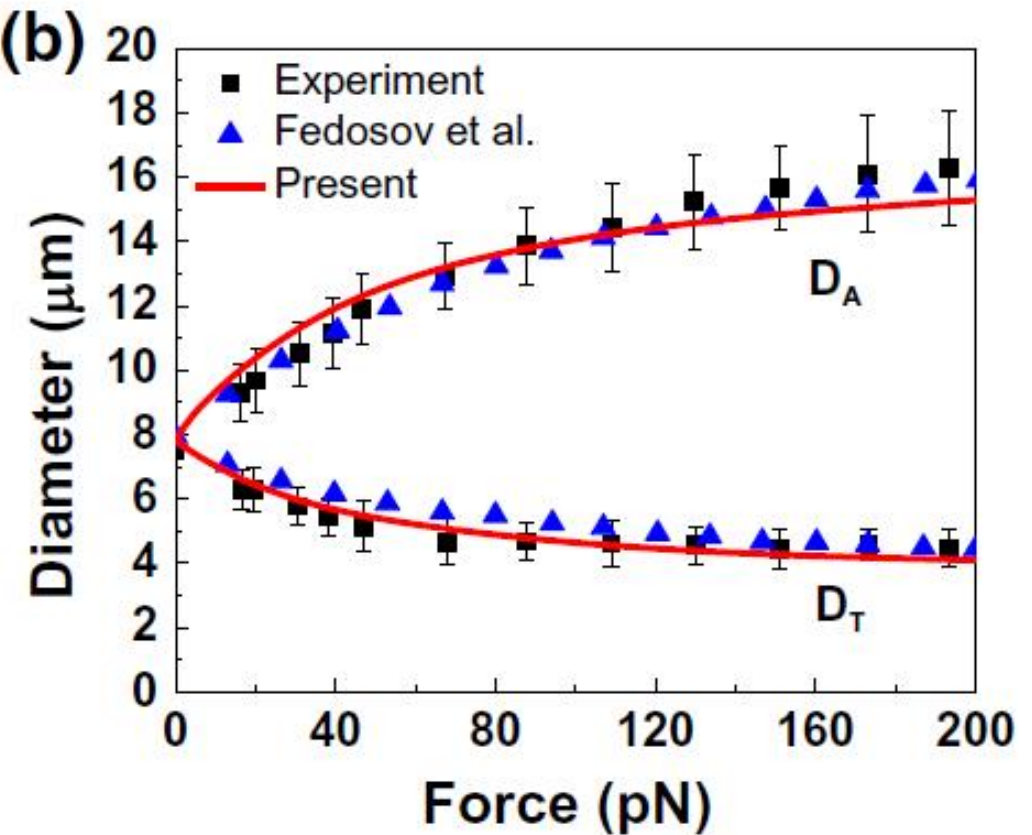
Force = 68 pN



Force = 151 pN



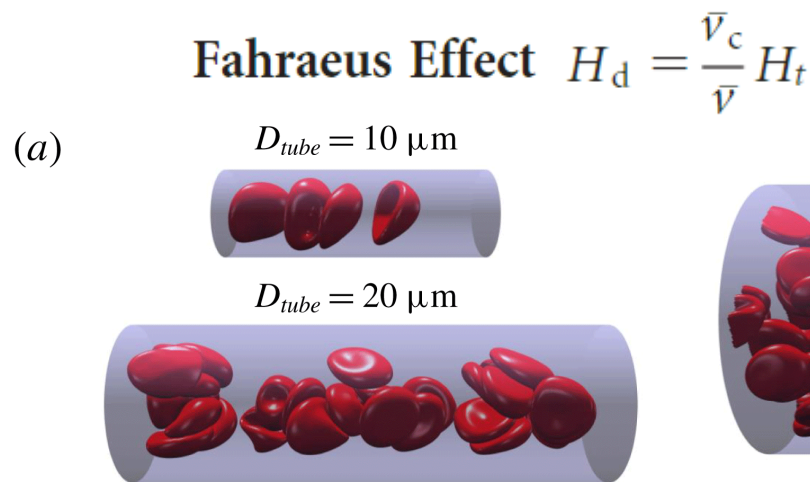
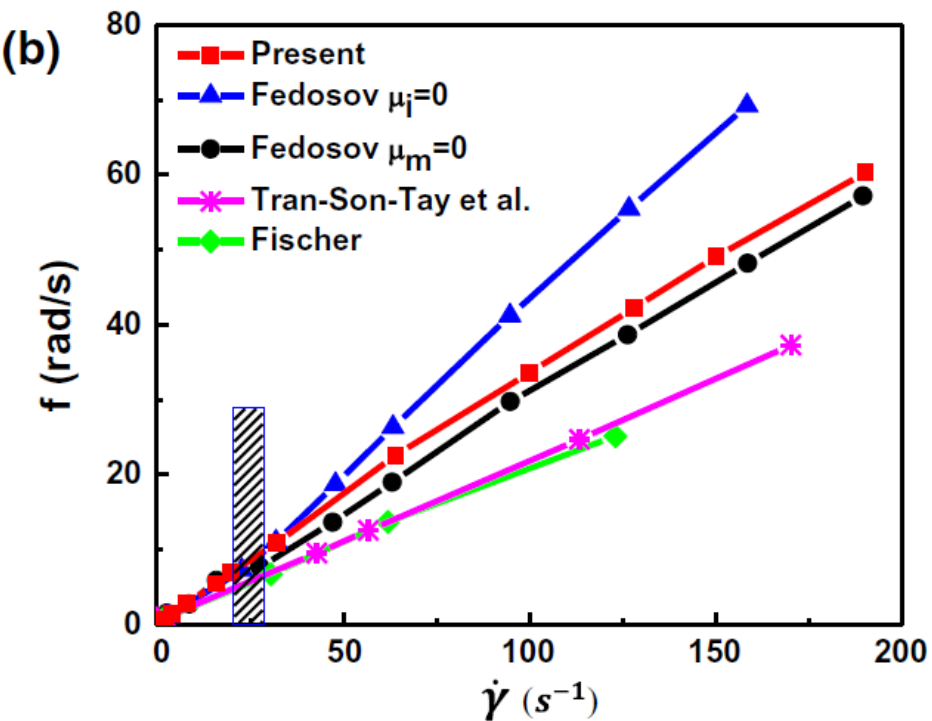
(b)



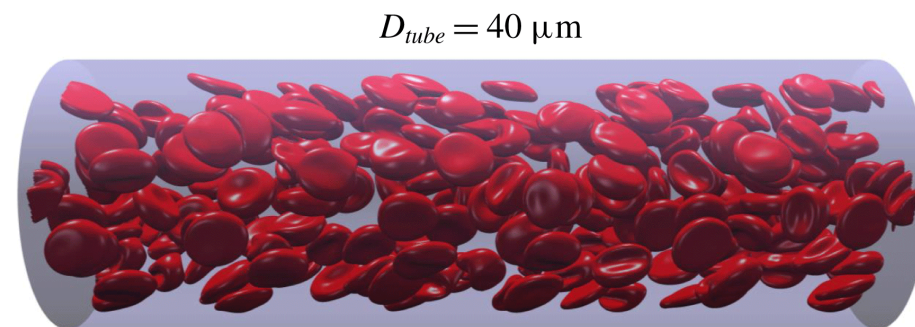
Stretching test of a single RBC. **a** Configuration of stretched RBC with different applied forces. **b** Diameters of RBC along stretching direction and transverse direction, denoted by D_A and D_T , respectively. The experimental results are reproduced with permission from Suresh S et al. Acta Biomater 23:S3–S15, 2015.

Tank-treading and tumbling a single RBC in simple shear flow

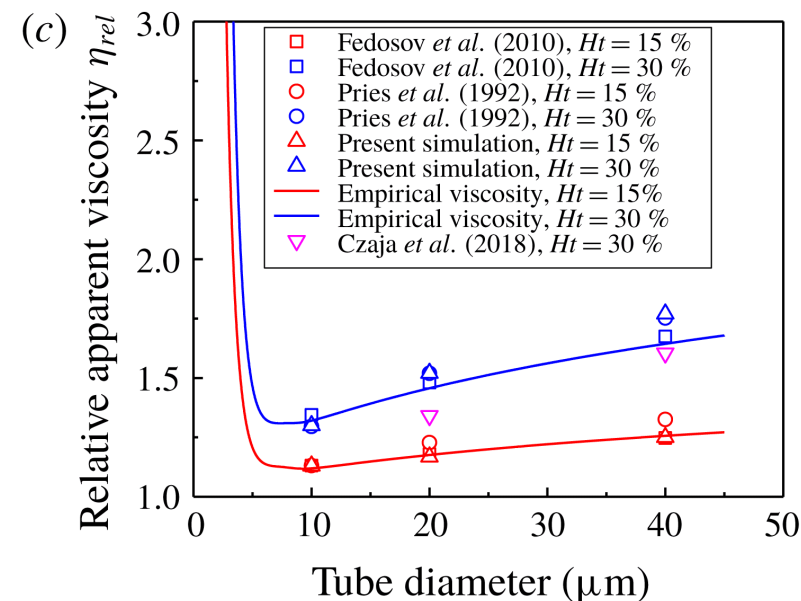
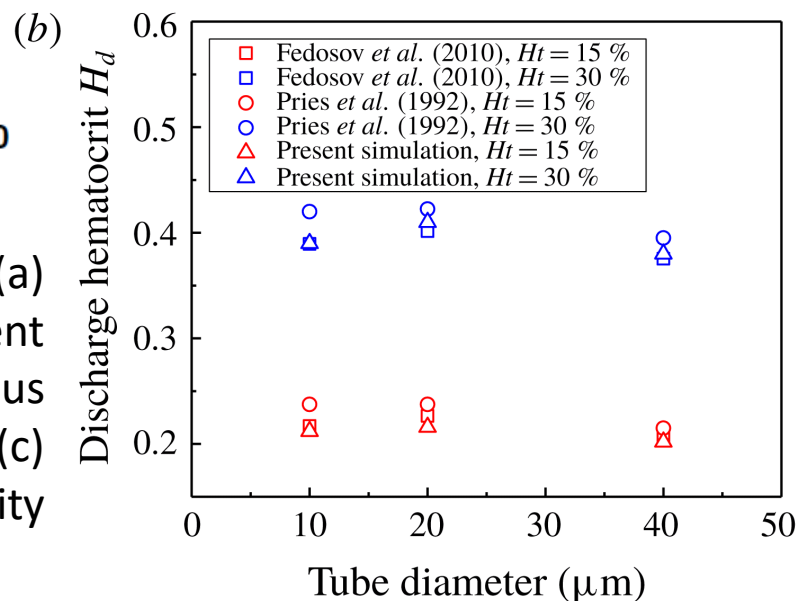
Fahraeus-Lindqvist Effect



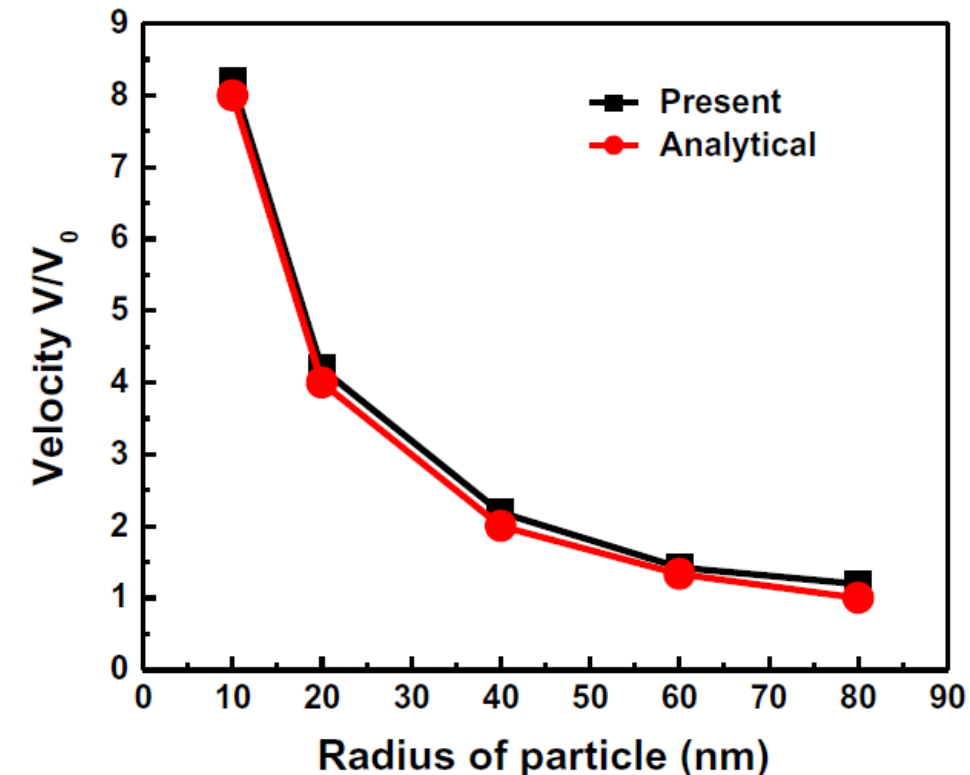
$$\eta_{app} = \frac{\pi \Delta P D^4}{128 Q L} = \frac{\Delta P D^2}{32 \bar{v} L} \quad \eta_{rel} = \frac{\eta_{app}}{\eta_s}$$



Fahraeus and Fahraeus-Lindqvist effects. (a) Snapshots to show the tube flow with different diameters under hematocrit 15%. (b) Fahraeus effect: discharge hematocrit comparison. (c) Fahraeus-Lindqvist effect: relative viscosity validation.

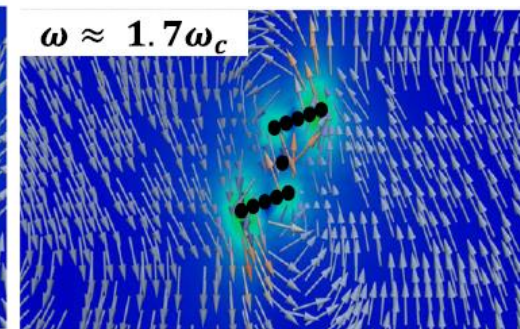
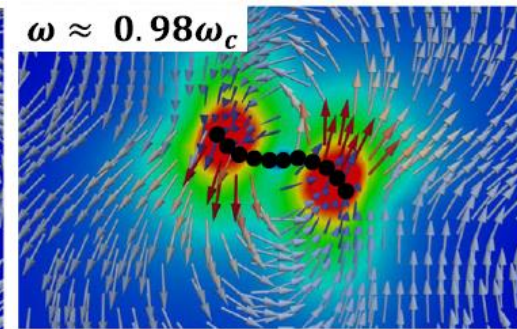
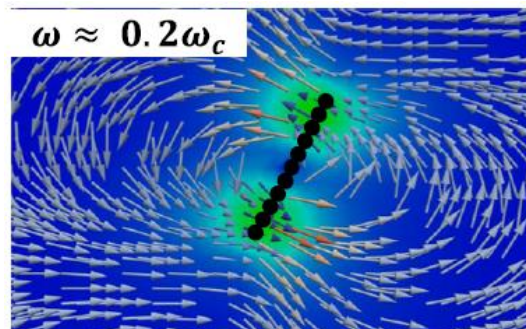
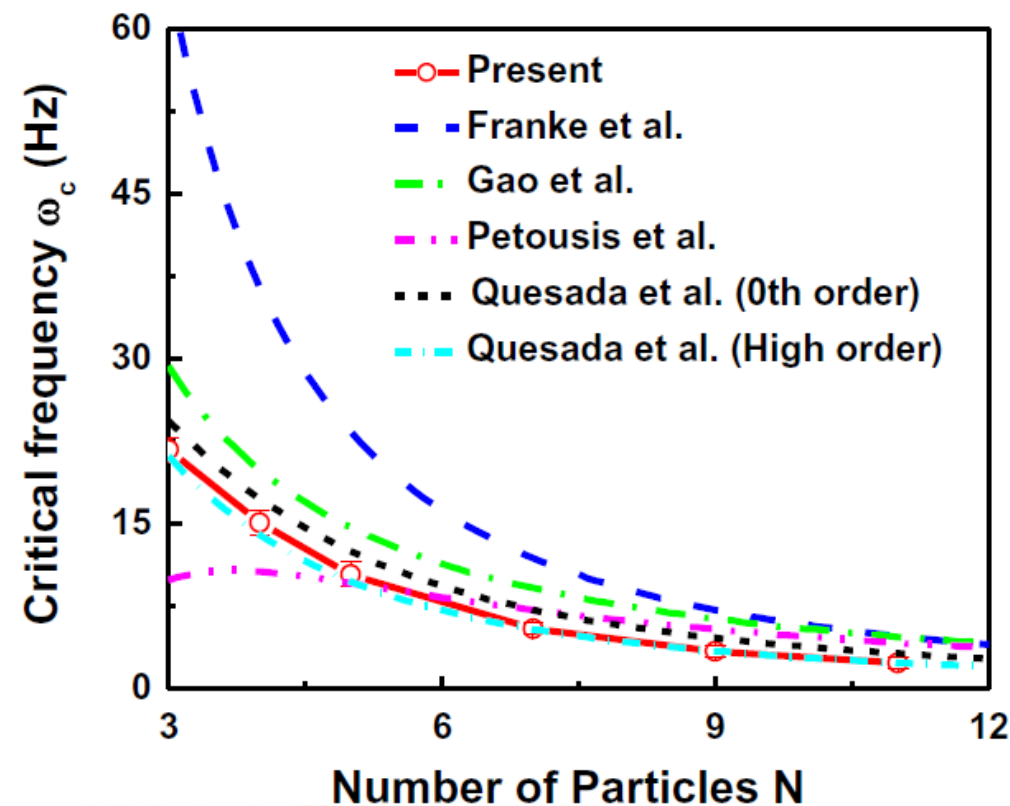


Moving of a single magnetic particle under non-uniform external magnetic field

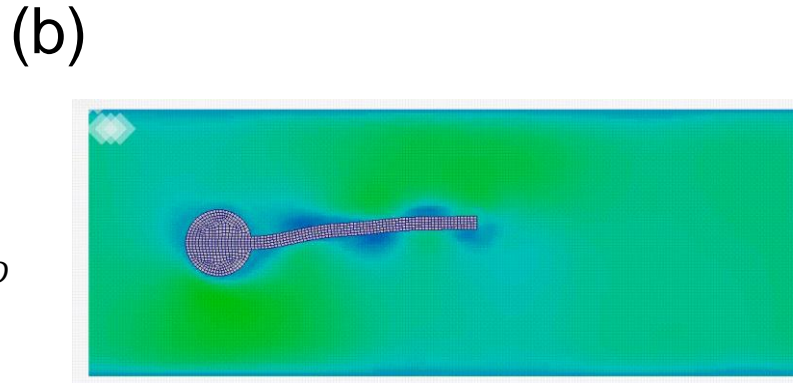
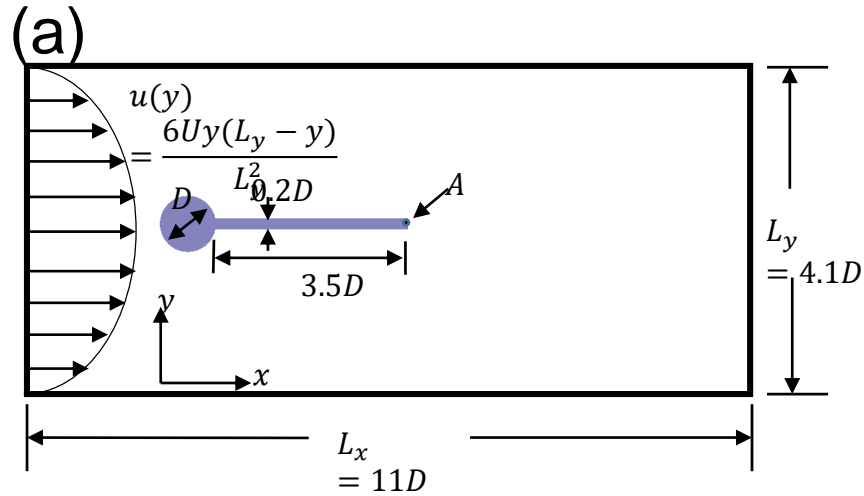


$$V_i = \frac{F_i^B}{6\pi\mu a}$$

Breakup of magnetic chain in rotating magnetic field

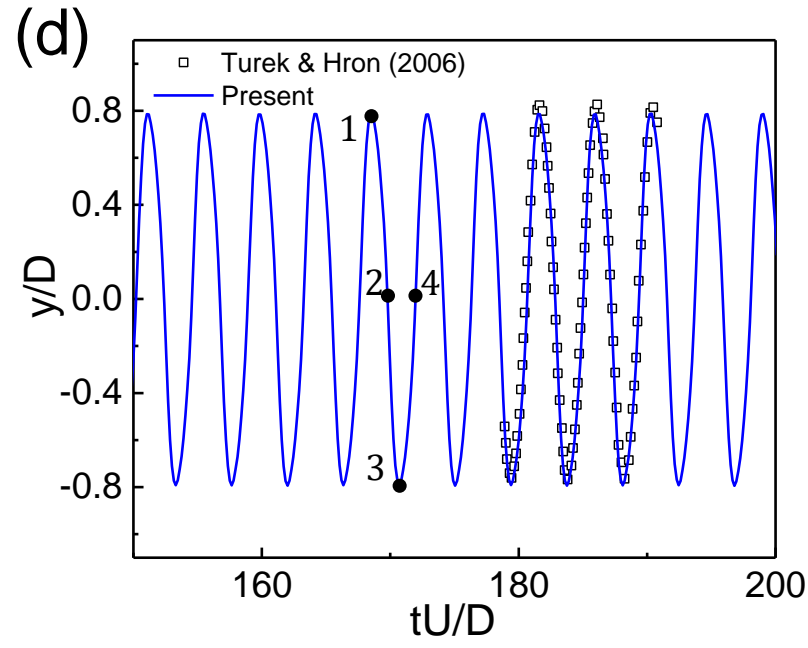
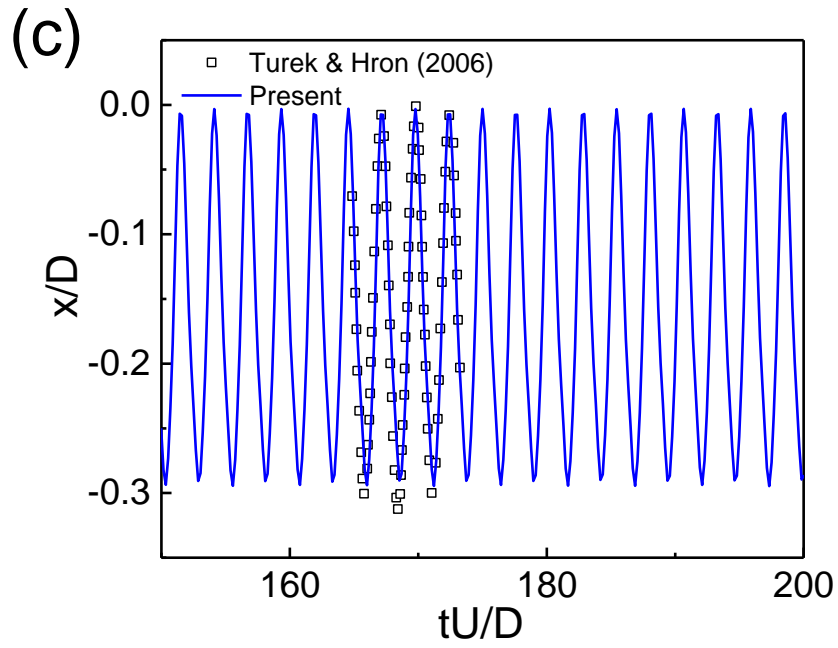


Flow-induced flapping of an elastic 2D beam behind a cylinder

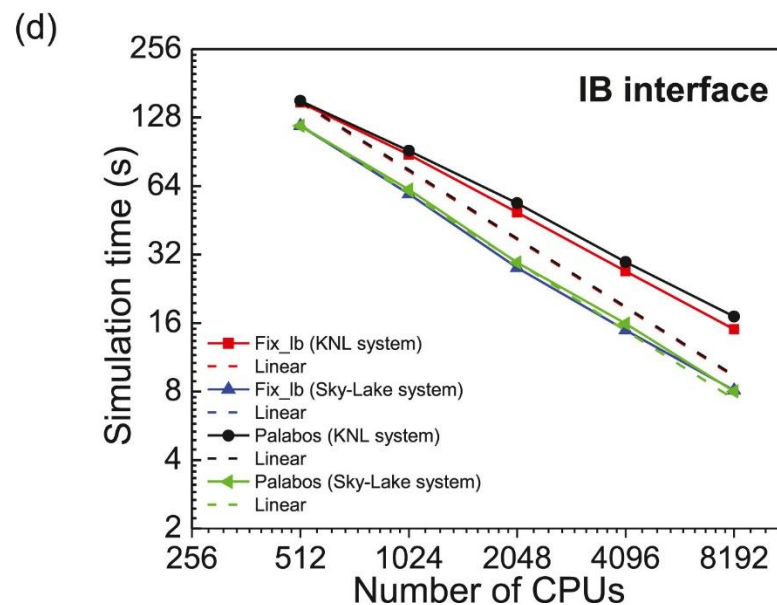
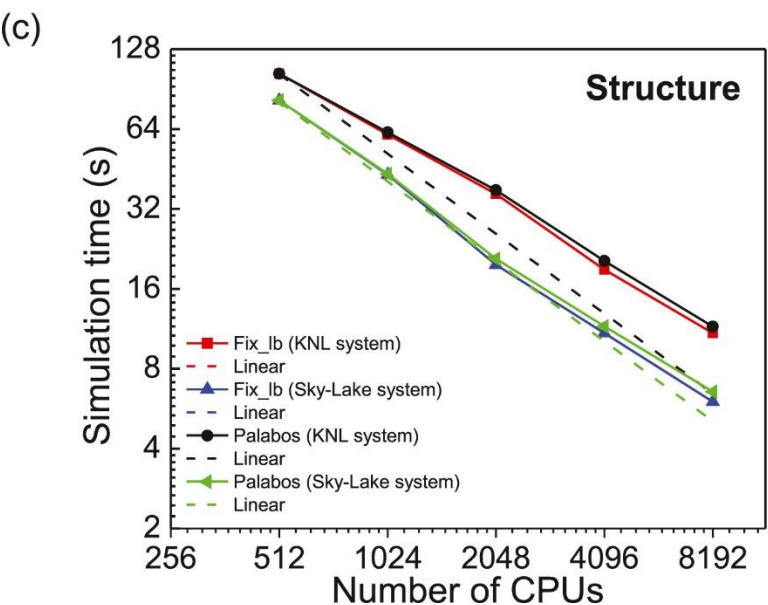
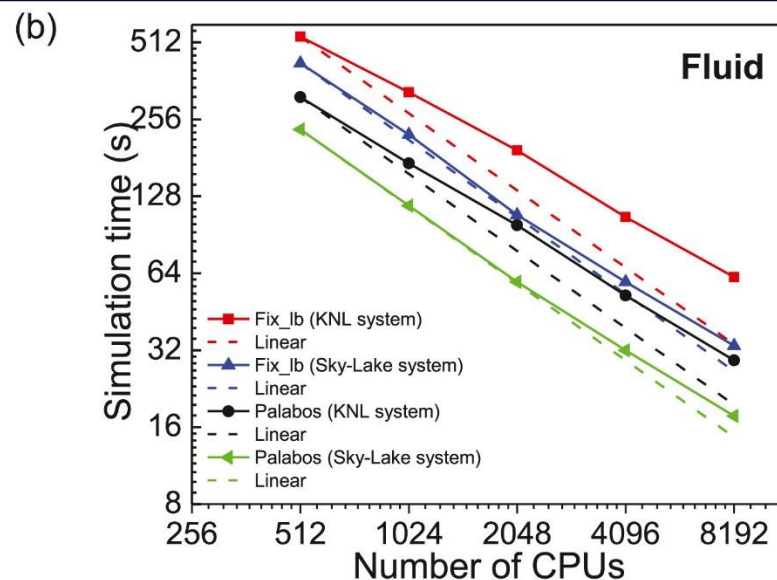
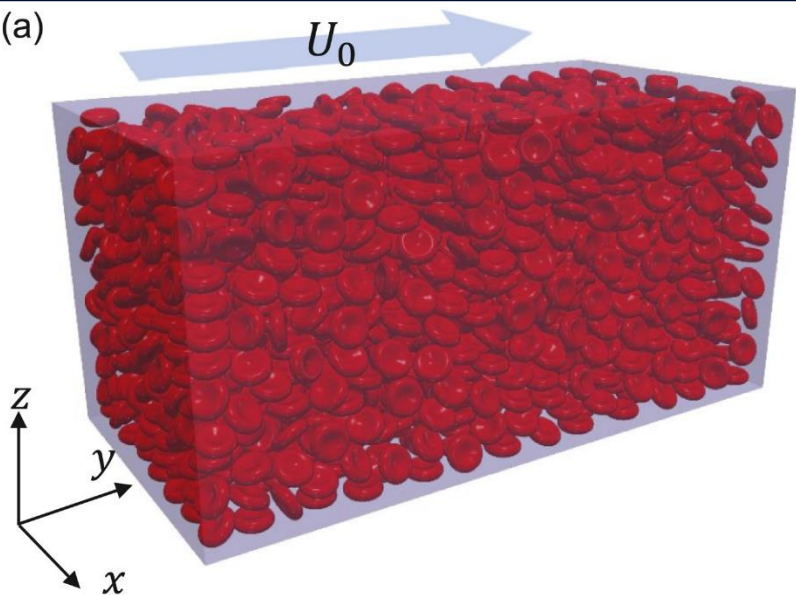


$St = fU/D$ Oscillating behavior

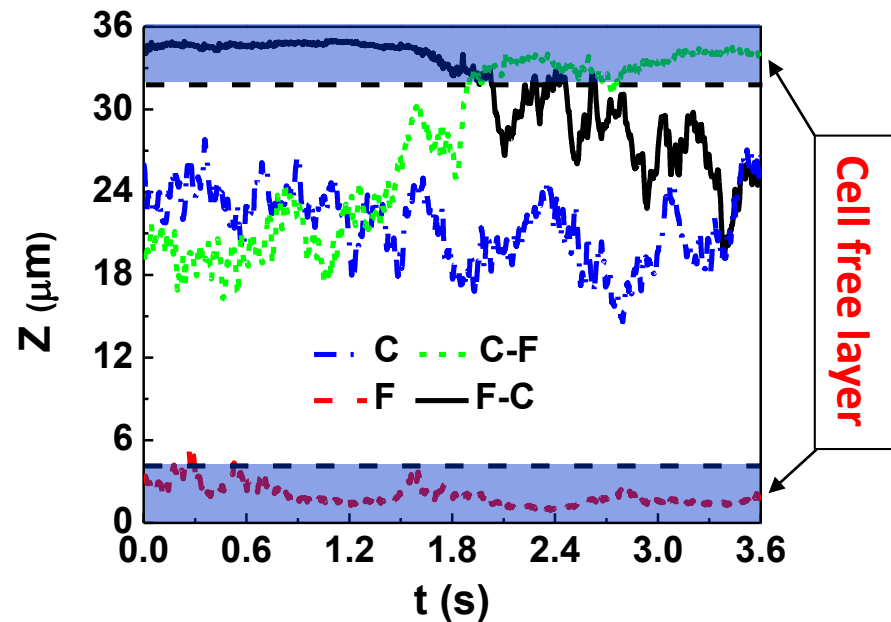
$C_D = F_x / (0.5\rho U^2 D)$ Drag coefficient



Works	Amplitude	Strouhal number	Drag coefficient
Turek and Hron (2006)	0.83	0.19	4.13
Tian et al. (2014)	0.78	0.19	4.11
Lin et al. (2019)	0.81	0.19	4.10
Present	0.79	0.19	4.10

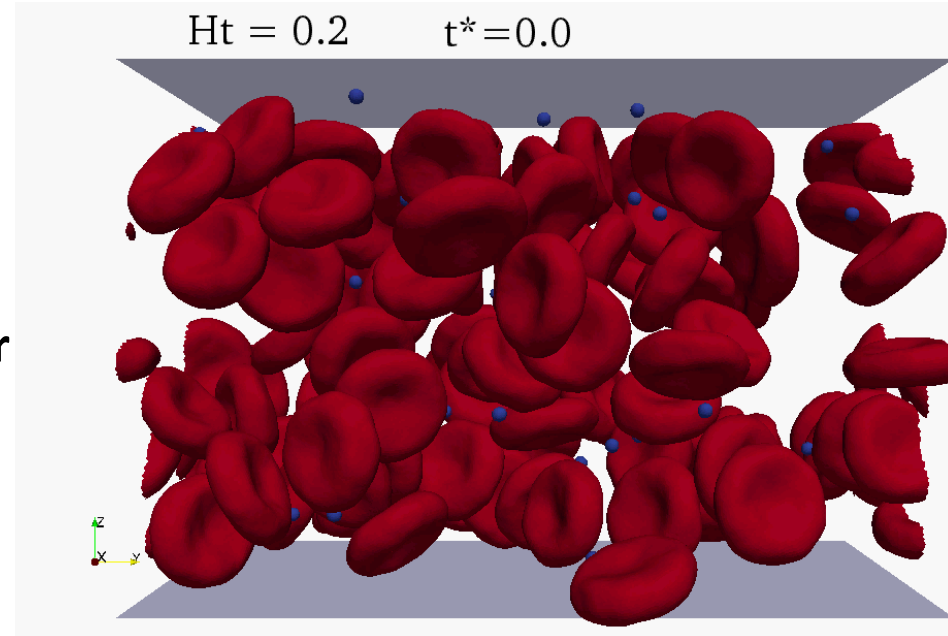


The computational efficiency is examined by estimating the time consumption used to run 2000 steps within present program. (a) Model of large-scale blood flow simulations with 2000 red blood cells. Separate simulation times of (b) fluid part, (c) structure part, and (d) IB interface part for running time steps in different systems with different solvers.



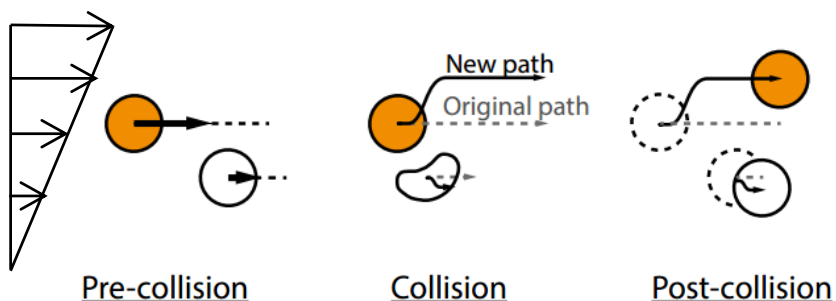
Four types of motion

- (A) C: stay in center region
- (B) F: stay in cell free layer
- (C) C-F: marginate from center to cell free layer
- (D) F-C: demarginate from cell free layer to center region

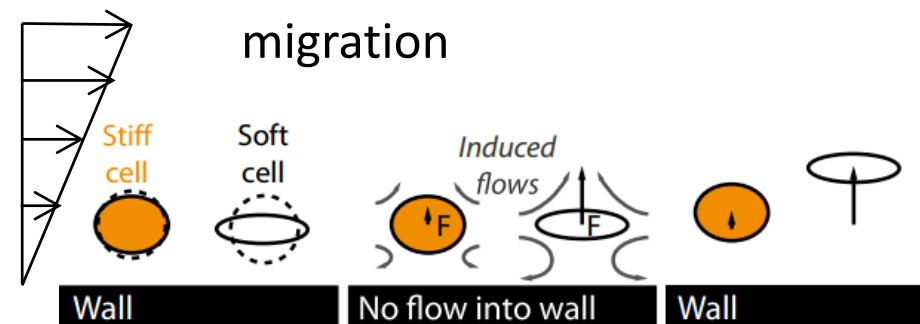


$$\Pi = \frac{n_f(t) - n_f(0)}{N - n_f(0)}$$

Particle-particle collisions



Deformation induced migration



❑ Anomalous vascular dynamics of nanoworms within blood Flow

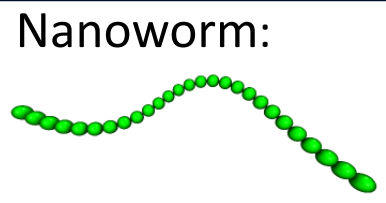
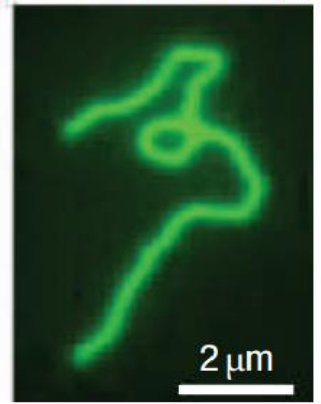
Passive targeting: Size, Shape and Stiffness

❑ Adhesion effect on margination of elastic micro-particles

❑ Motion of particle under external magnetic field

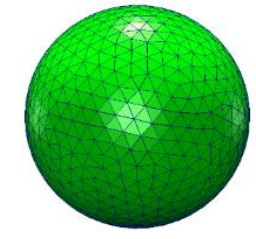
Circulation: Vascular dynamics of nanoworms in blood flow

Fluorescence microscopy



$$U_{\text{stretching}}^P = k_s^P (l - l_0)^2$$

$$U_{\text{bending}}^P = \kappa (\theta - \theta_0)^2$$



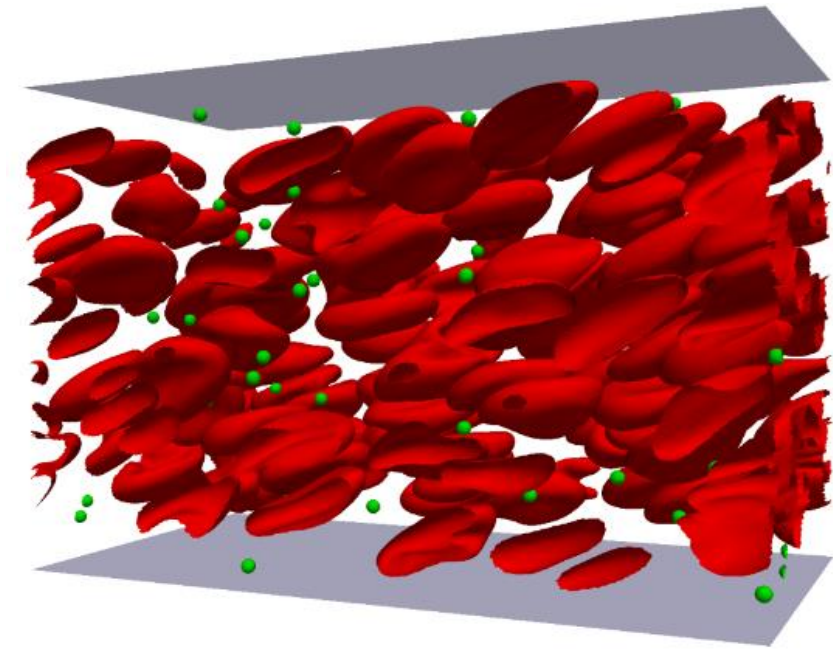
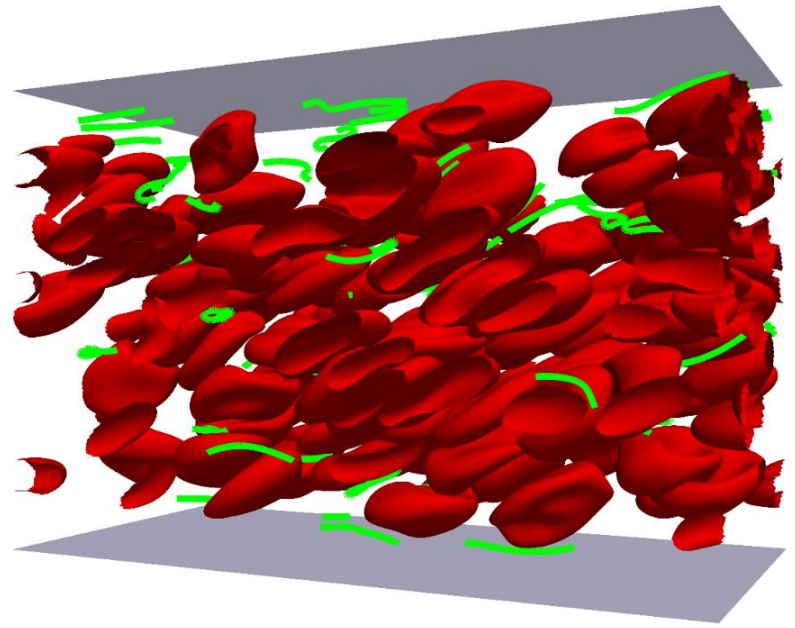
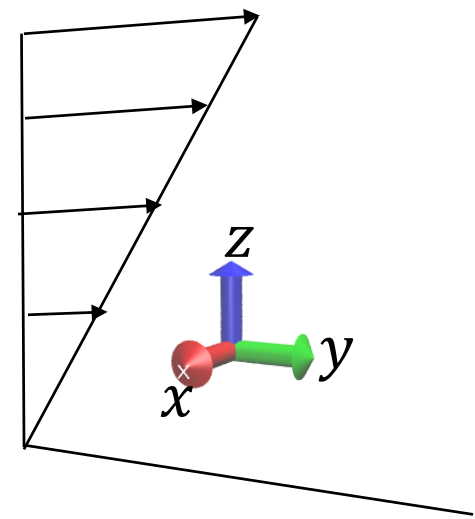
Sphere: 1 μm ($N_p=50$)

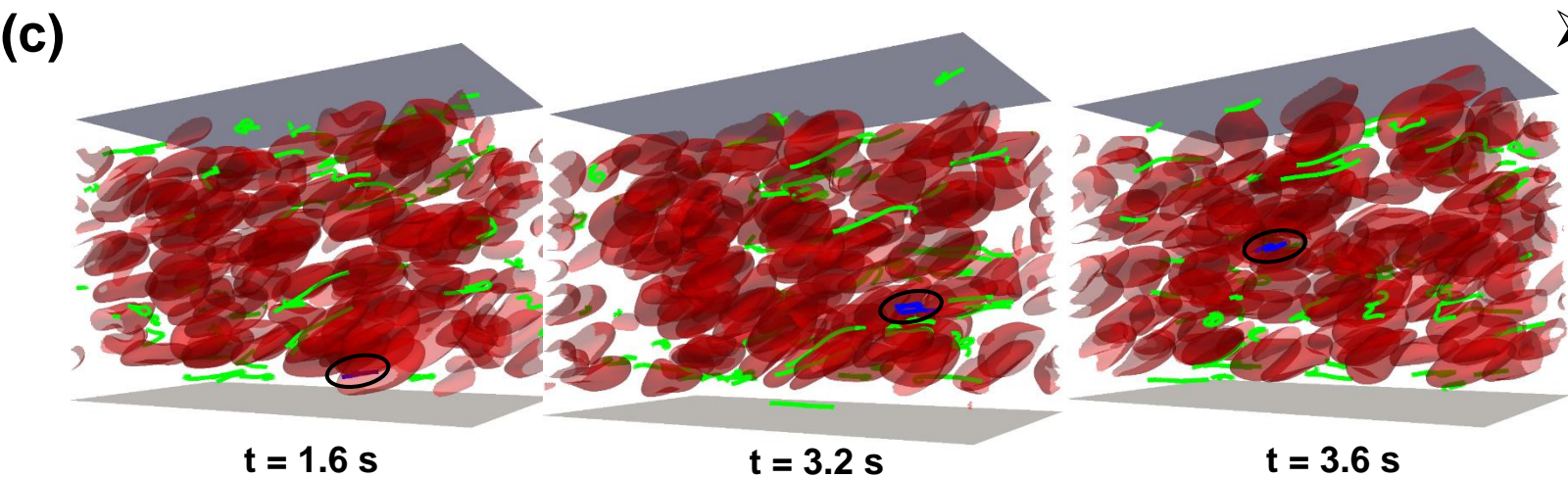
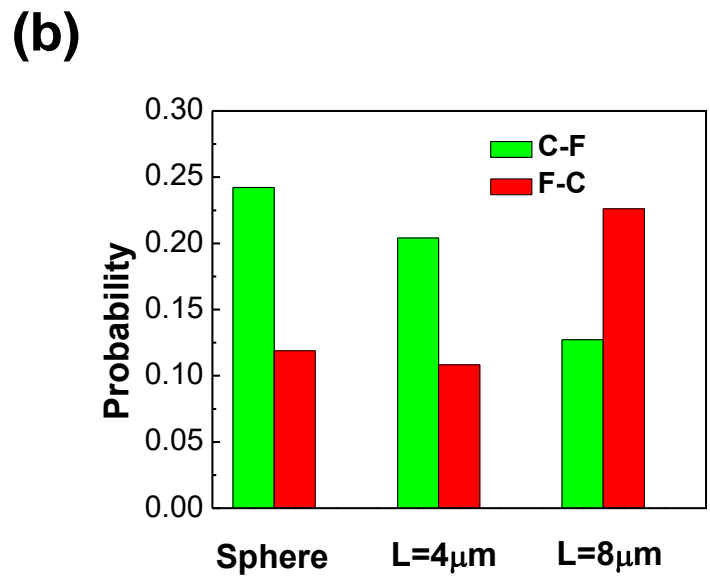
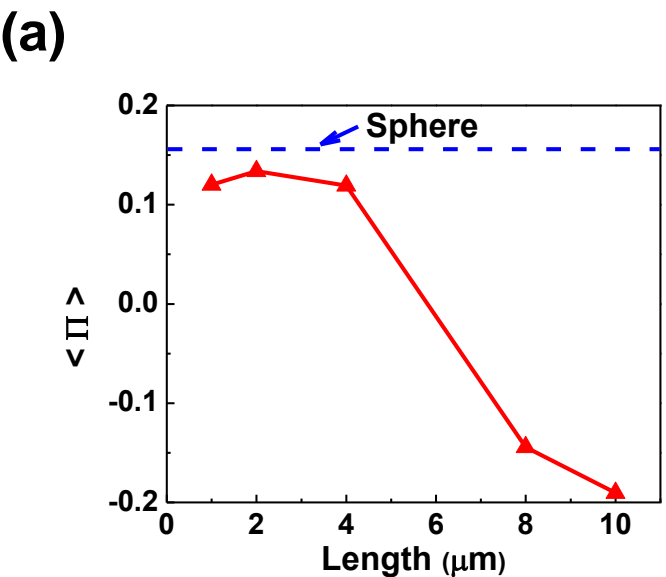
Length (μm)				
1	2	4	8	10

$$\mathbf{u} = \{0, \gamma z, 0\} \quad \dot{\gamma} = 248 \text{ s}^{-1}$$

$$L_x \times L_y \times L_z = 27\mu\text{m} \times 54\mu\text{m} \times 36\mu\text{m}$$

Ht: 20% ($N_R = 108$)



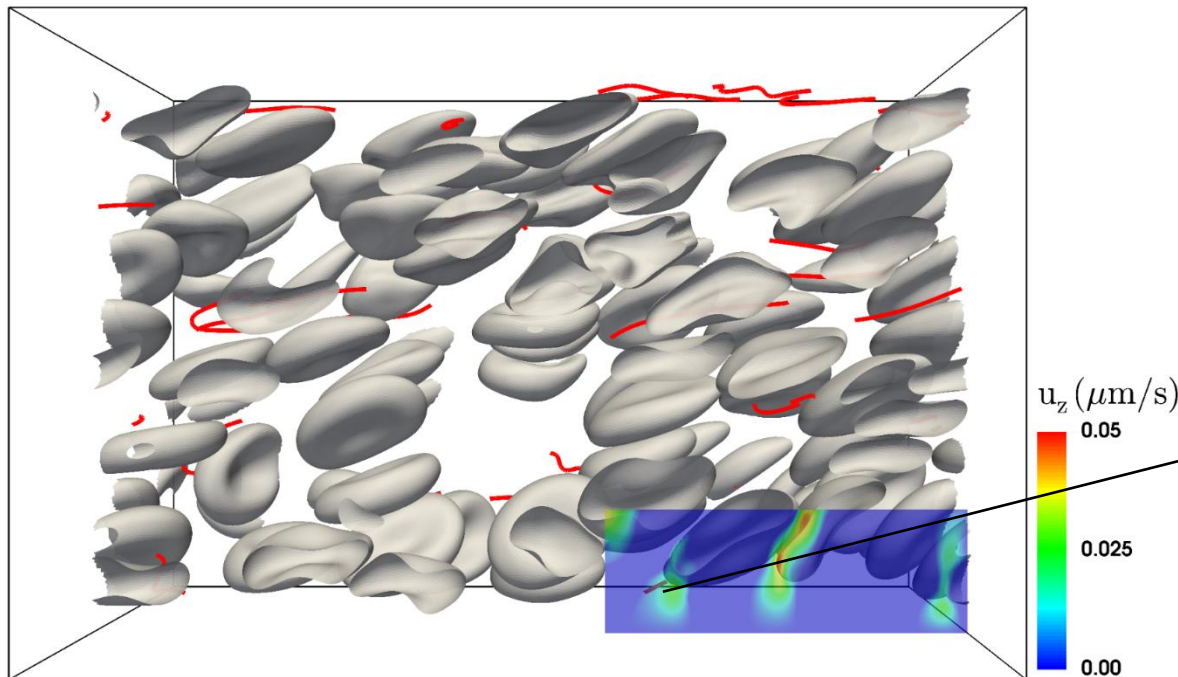
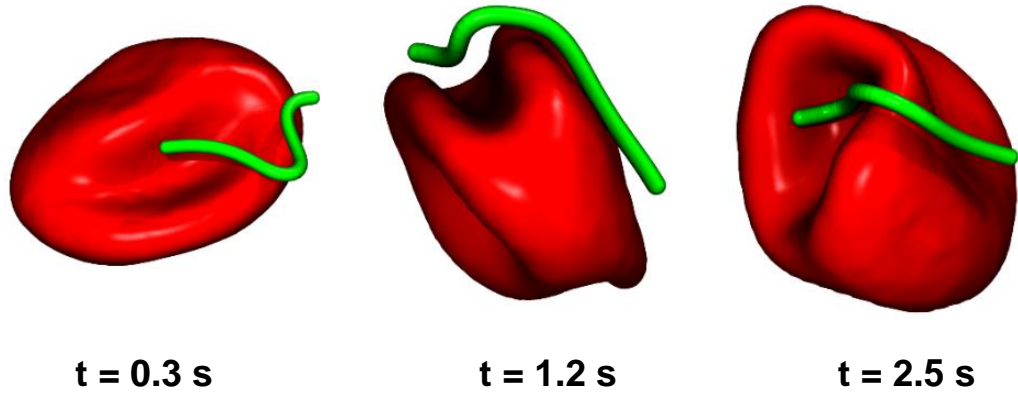


Results

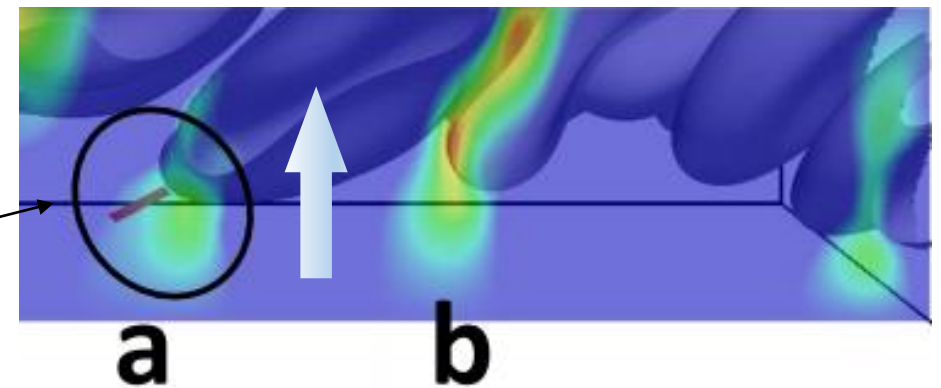
- Short nanoworms show margination behavior
- Margination probability of long nanoworms are negative

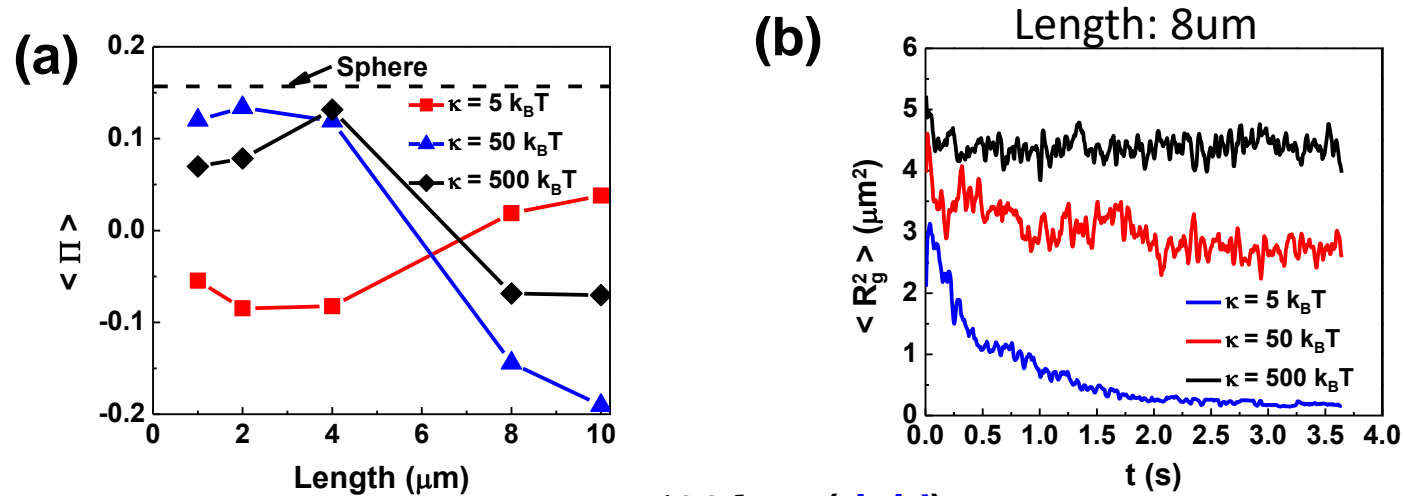
Reasons

- C-F motion dominates for short nanoworms
- F-C motion dominates for long nanoworms. Demargination outperforms margination.



- ❑ **Low Margination:** Flexible nanoworms deform to the same shape with RBCs and intertwine with them, moving along bulk flow.
- ❑ **Demargination:** Perturbation of fluid flow around RBCs due to deformation induces lateral flow, and drag the nanoworms to the center of channel.



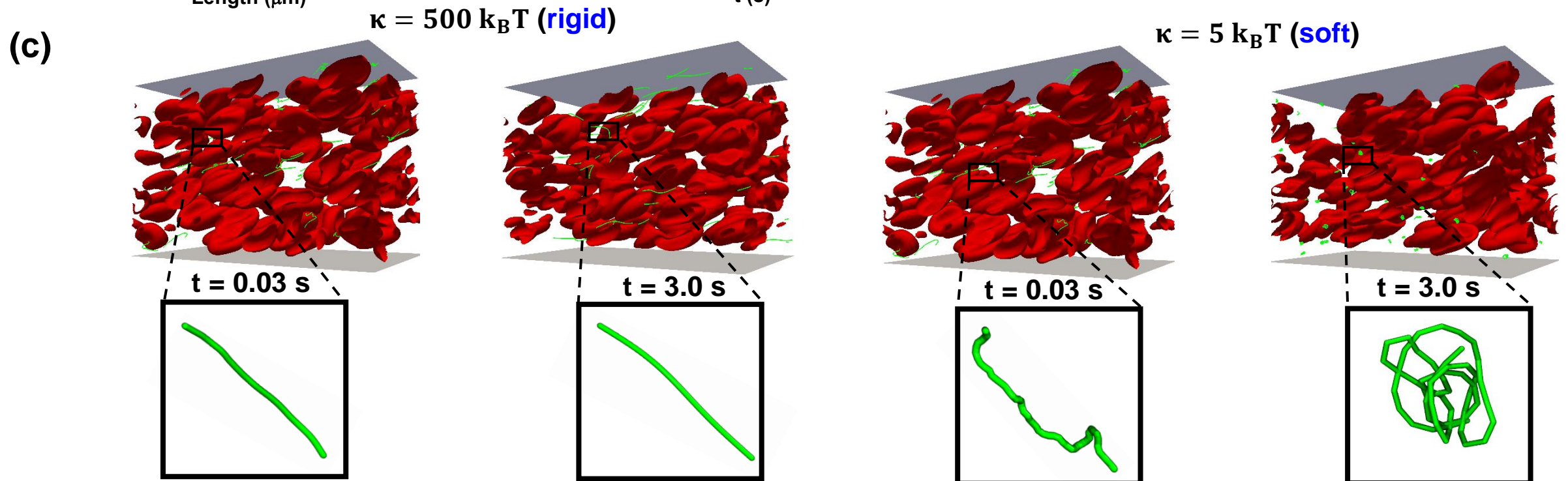


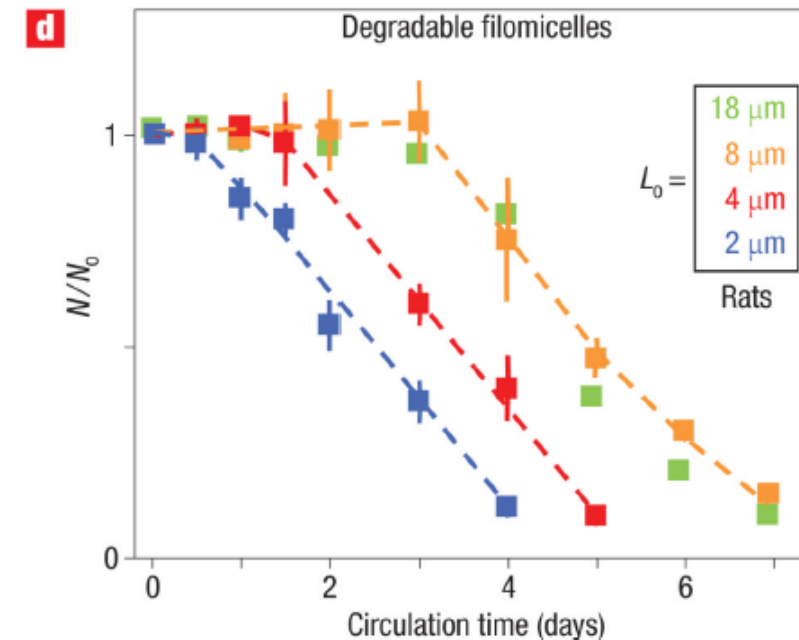
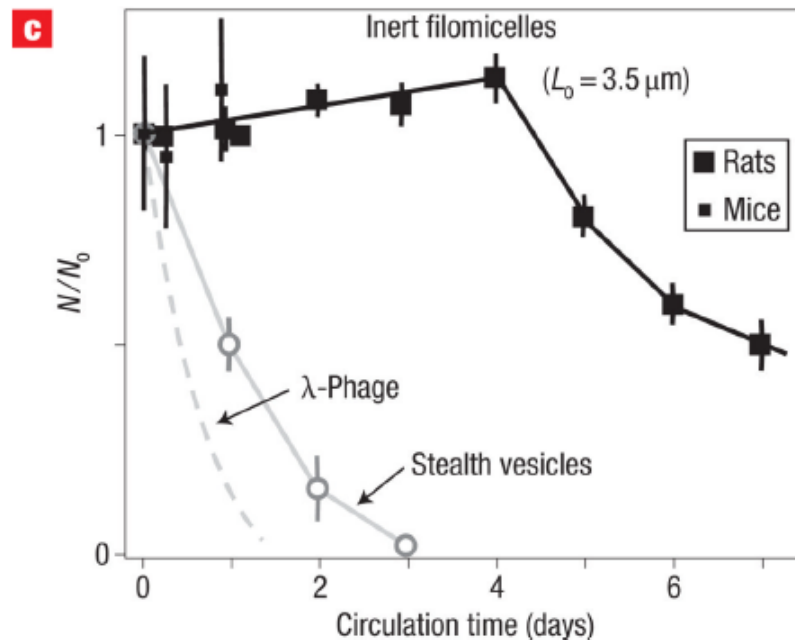
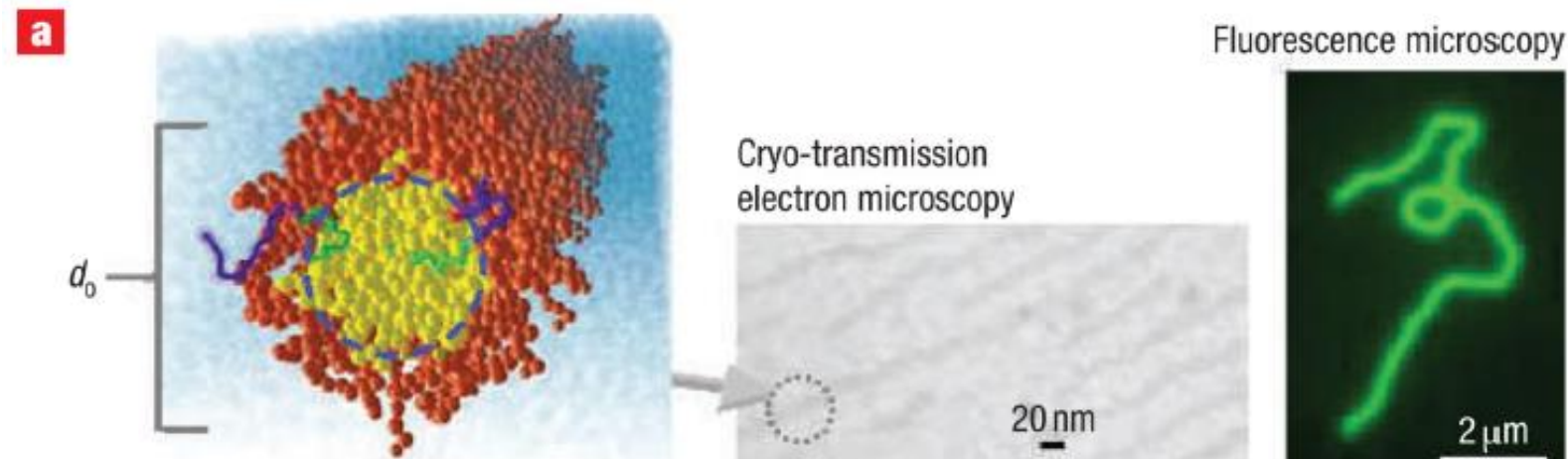
Size in space: radius of gyration $\langle R_g^2 \rangle$

Rigid: hard to deform to conformal to RBC

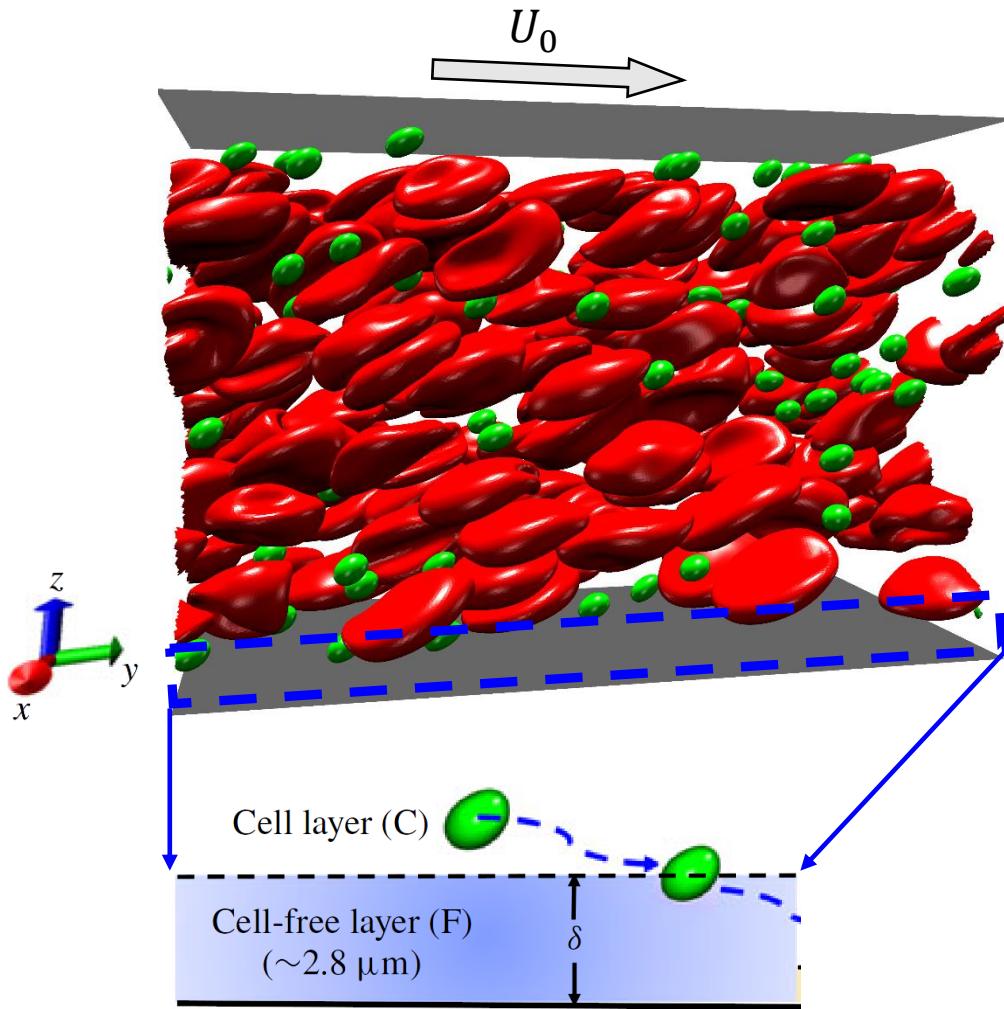
Semi-flexible: deform and circulate with RBC

Soft: collapse in flow





- Anomalous vascular dynamics of nanoworms within blood Flow
- **Adhesion effect on margination of elastic micro-particles**
 - Passive targeting: Stiffness and Adhesion (Surface)**
- Motion of particle under external magnetic field



$$L_z \times L_z \times L_z = 27 \times 54 \times 36 \mu\text{m}^3, \quad \gamma = \frac{U_0}{L_z} = 200 \text{ s}^{-1}$$

162 RBCs and 80 particles Volume fraction of RBC: 30%

Dimensionless numbers

capillary number $Ca = \mu \dot{\gamma} R / \mu_0$

Rigid

Soft

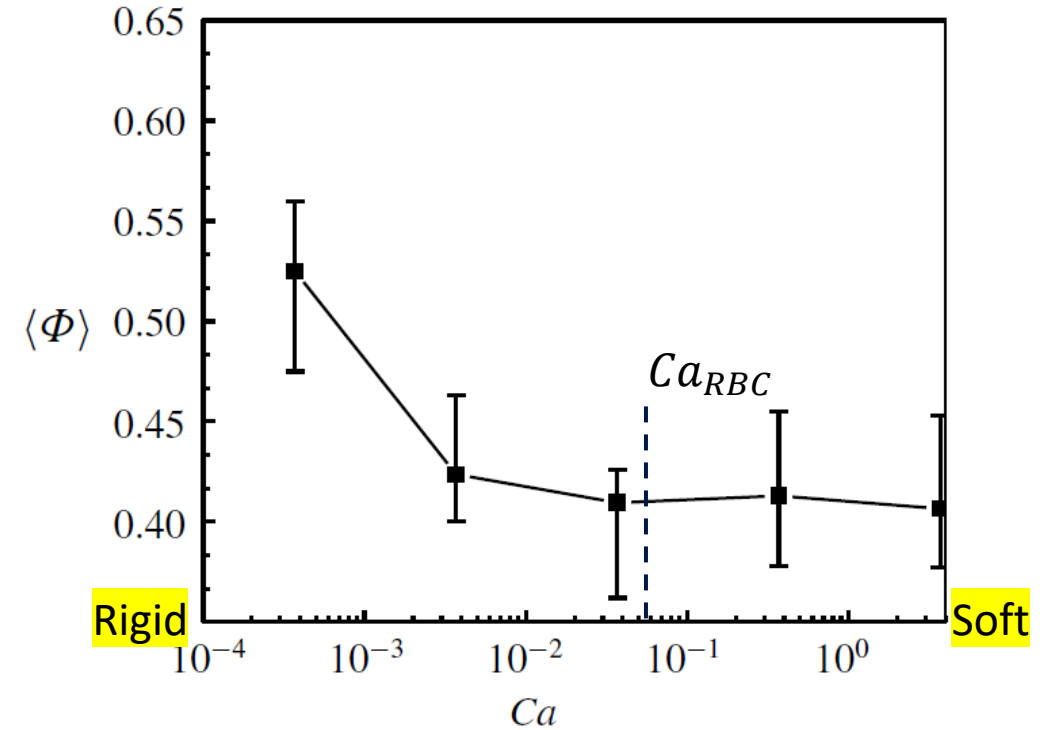
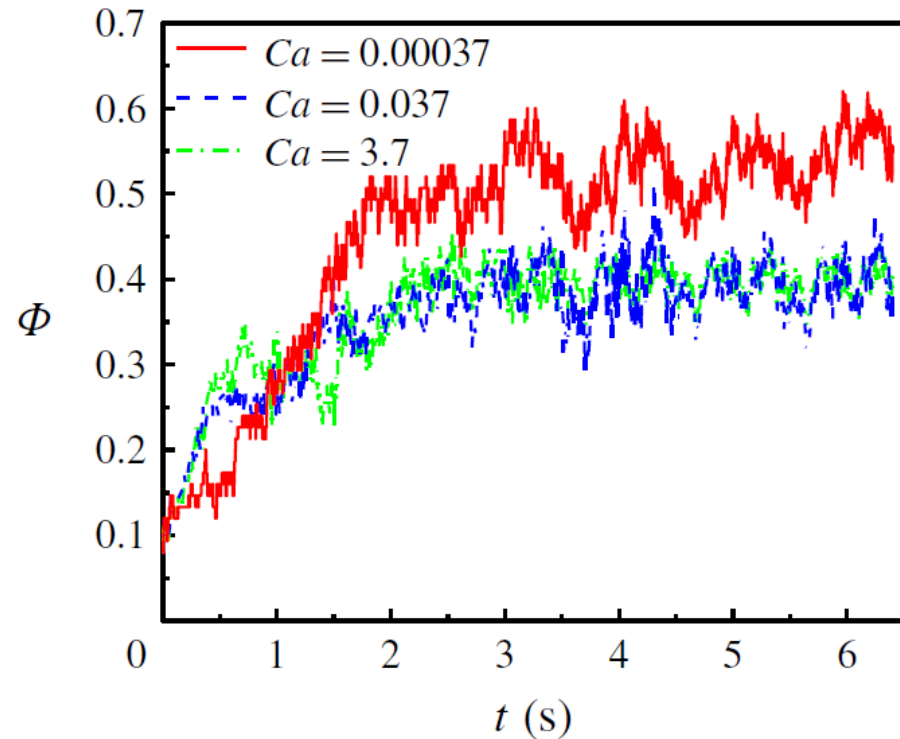
adhesion number $Ad = k_s / \mu \dot{\gamma} R$

Weak

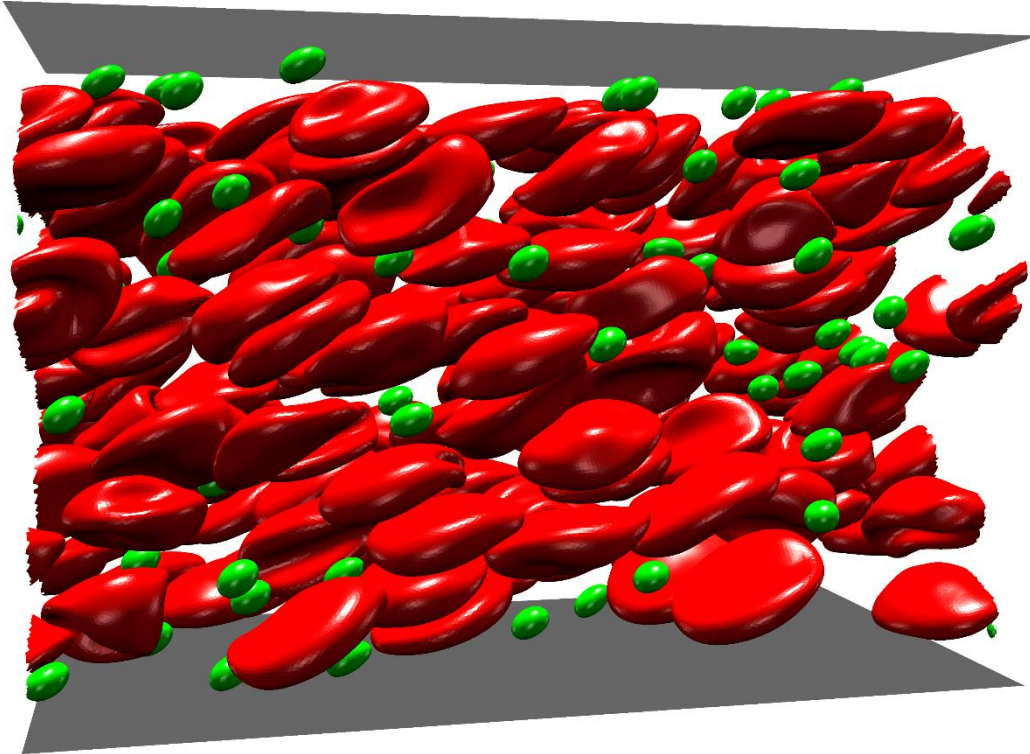
Strong

Margination Probability

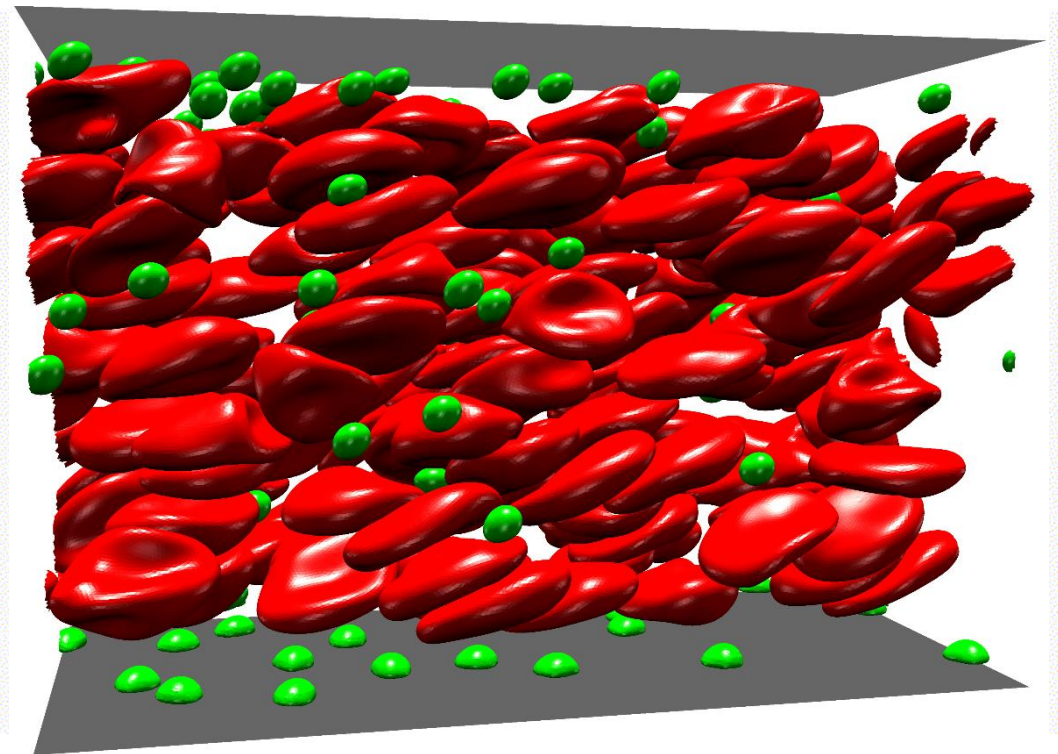
$$\Phi(t) = \frac{n_f(t)}{N}$$



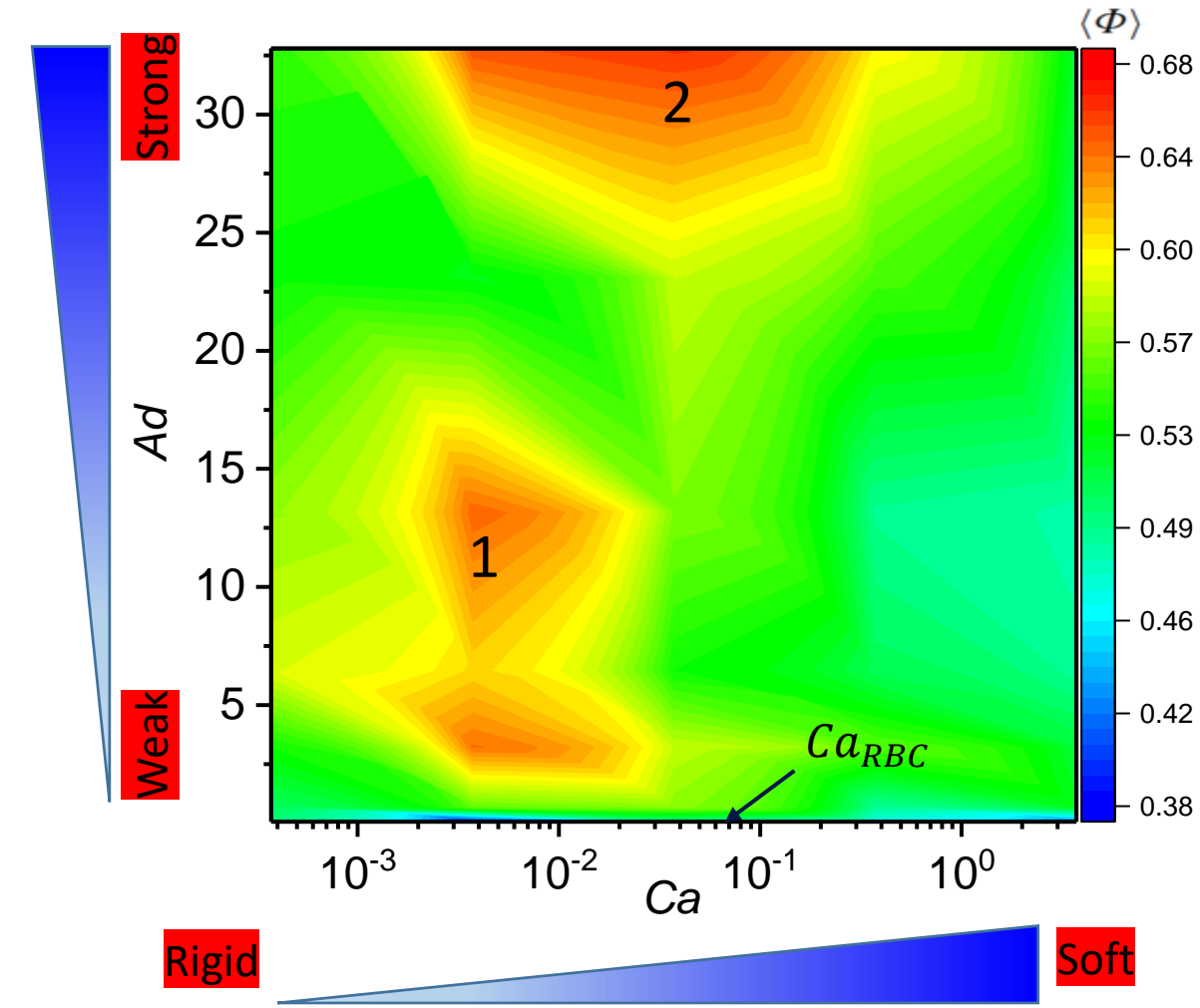
- Rigid particle has stronger margination (consistent with *Kumar & Graham, 2011*)
- Margination is independent on the stiffness when particle becomes soft enough



No adhesion



With adhesion



Two optimal regions (high probability)

(1) large stiffness and weak adhesion;

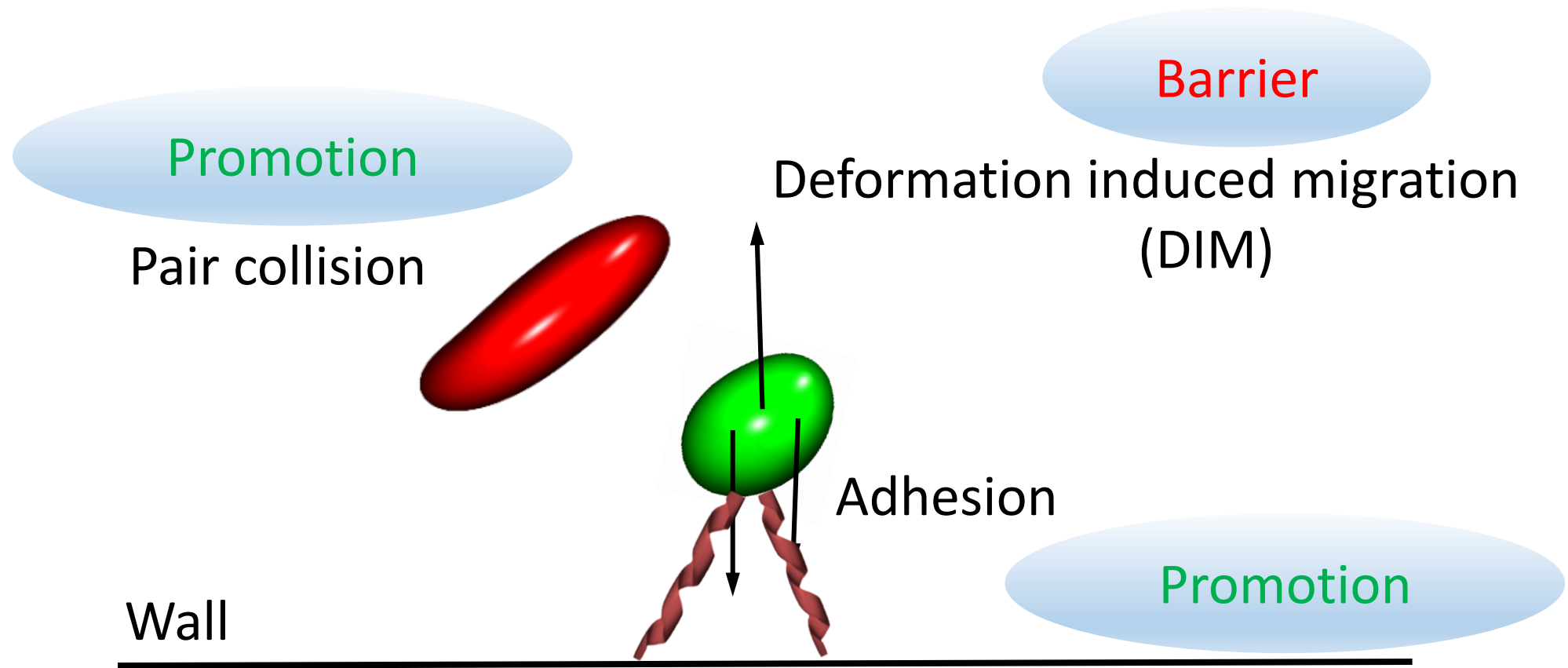
(2) Moderate stiffness and strong adhesion

Interplay of stiffness and adhesion

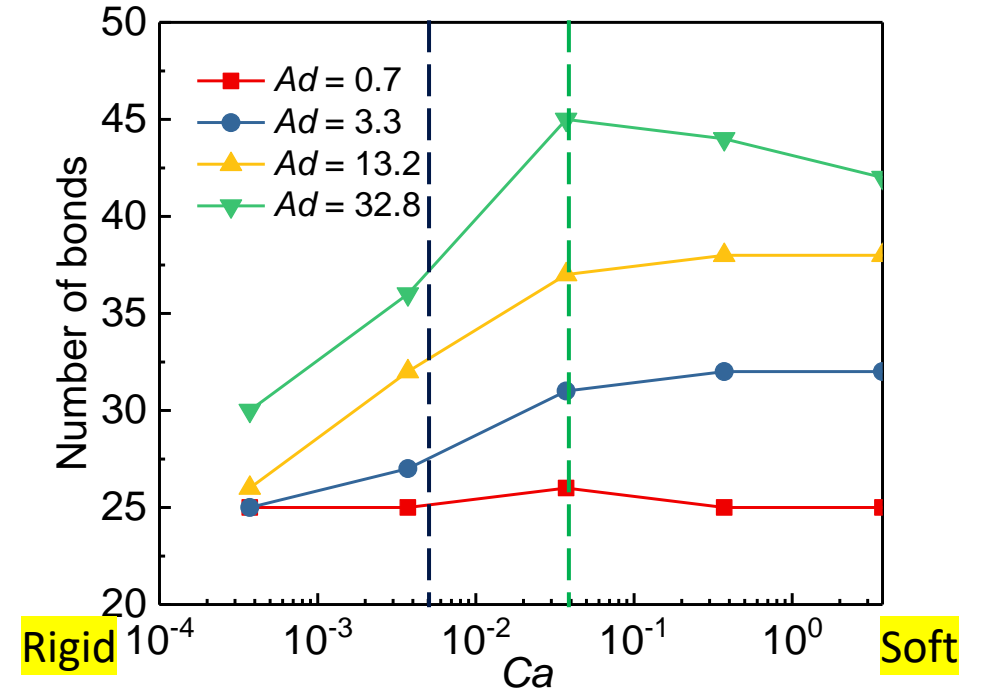
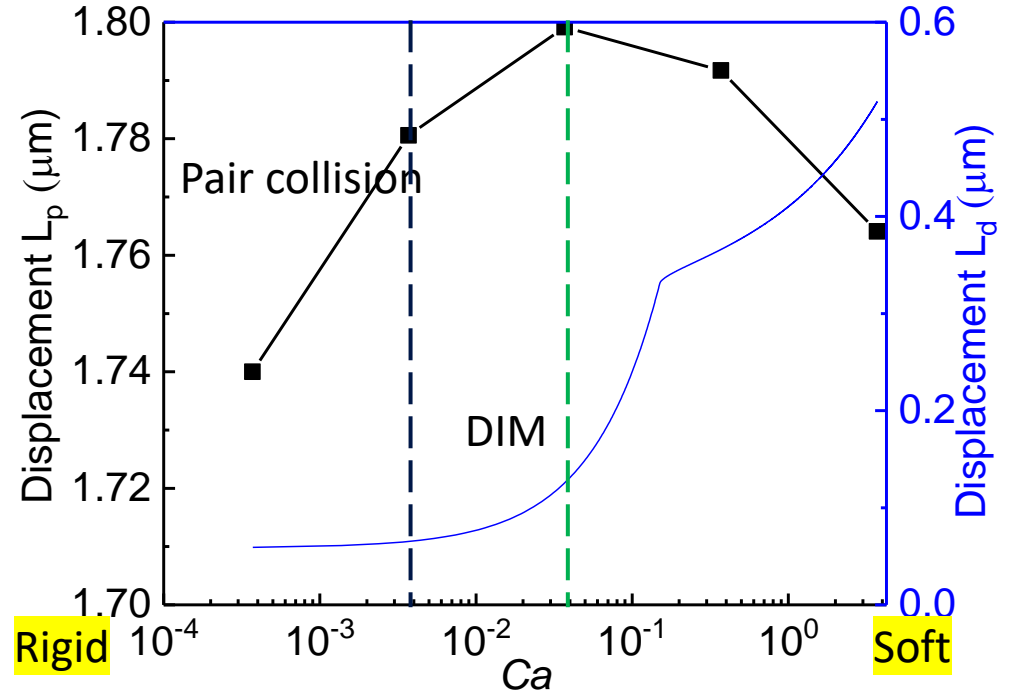
(1) Rigid or softer particle is not always better

(2) Stronger adhesion is also not better

What's the underlying mechanism?

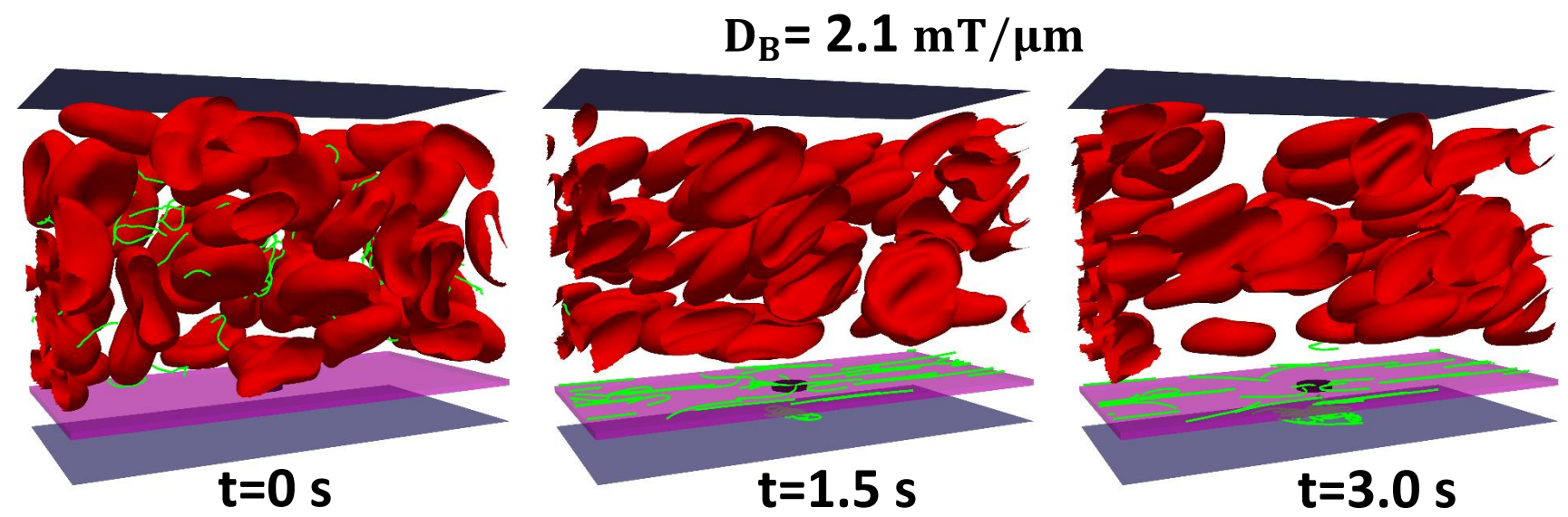
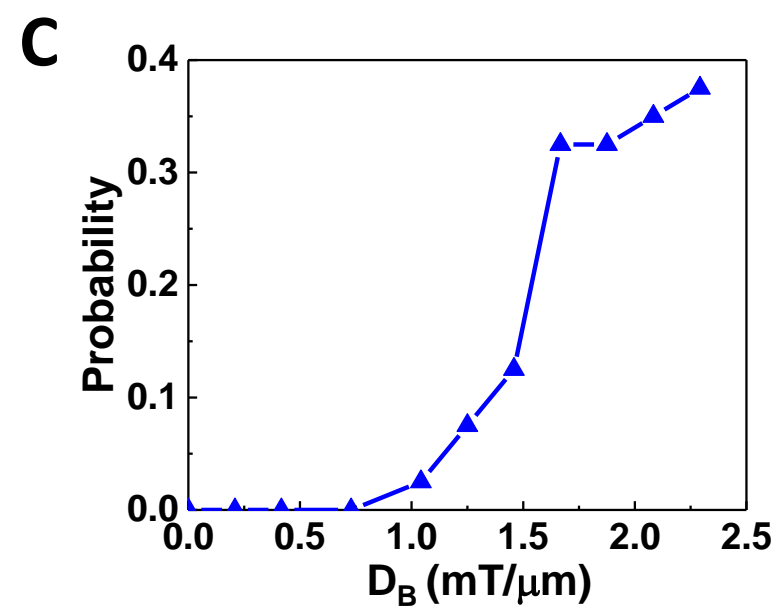
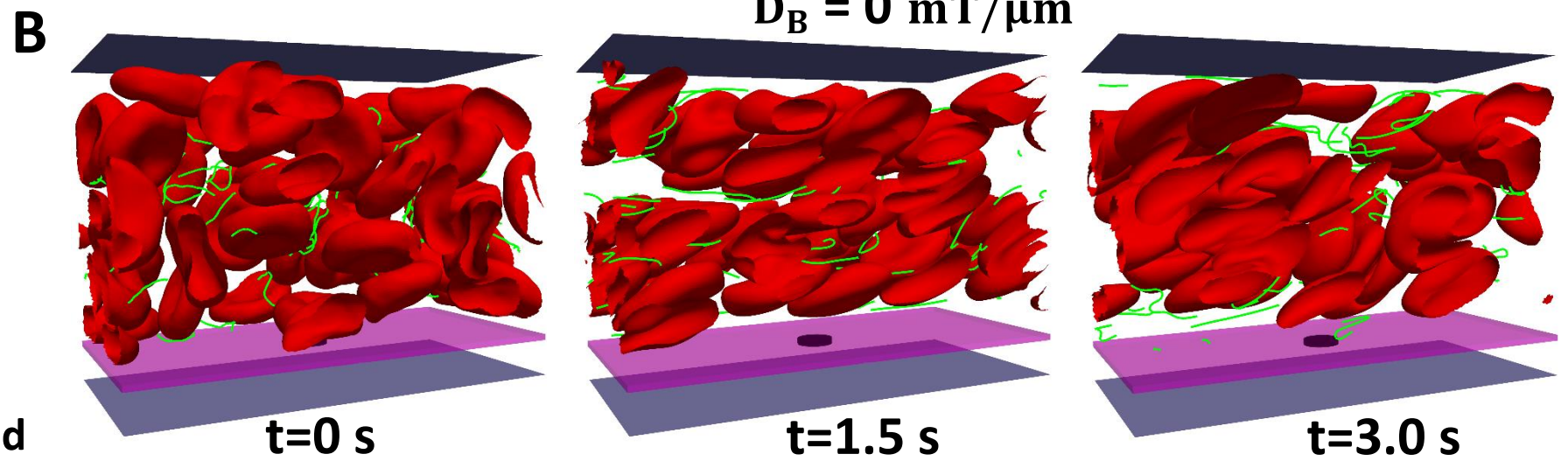
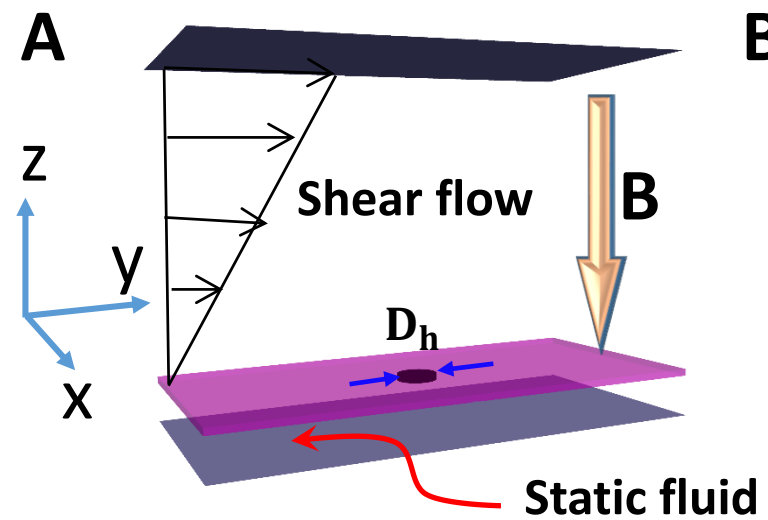


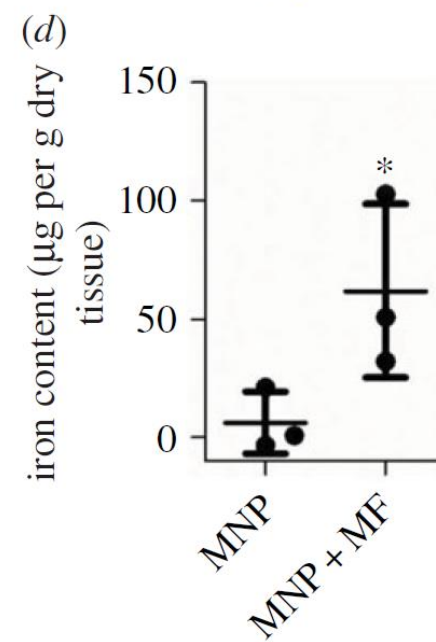
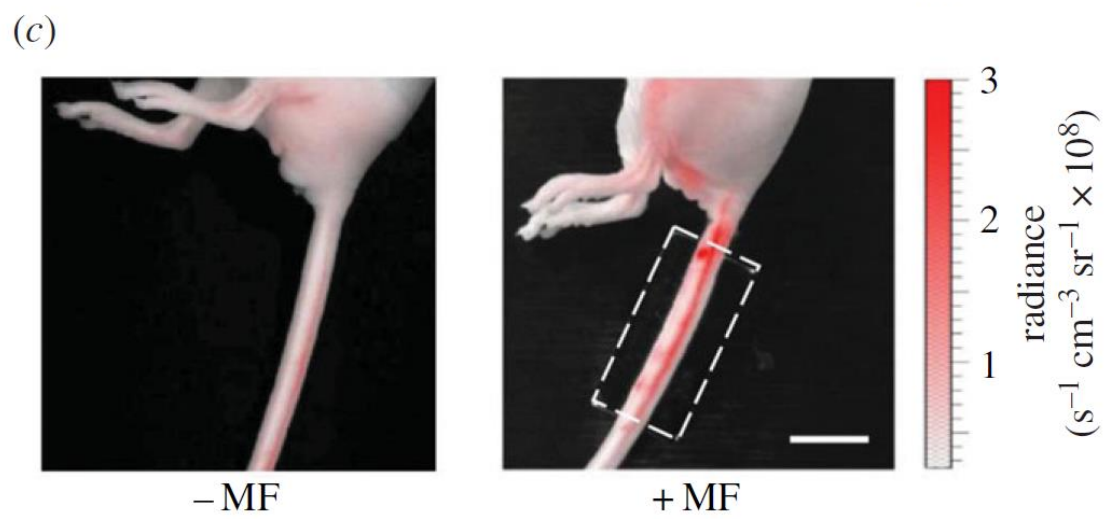
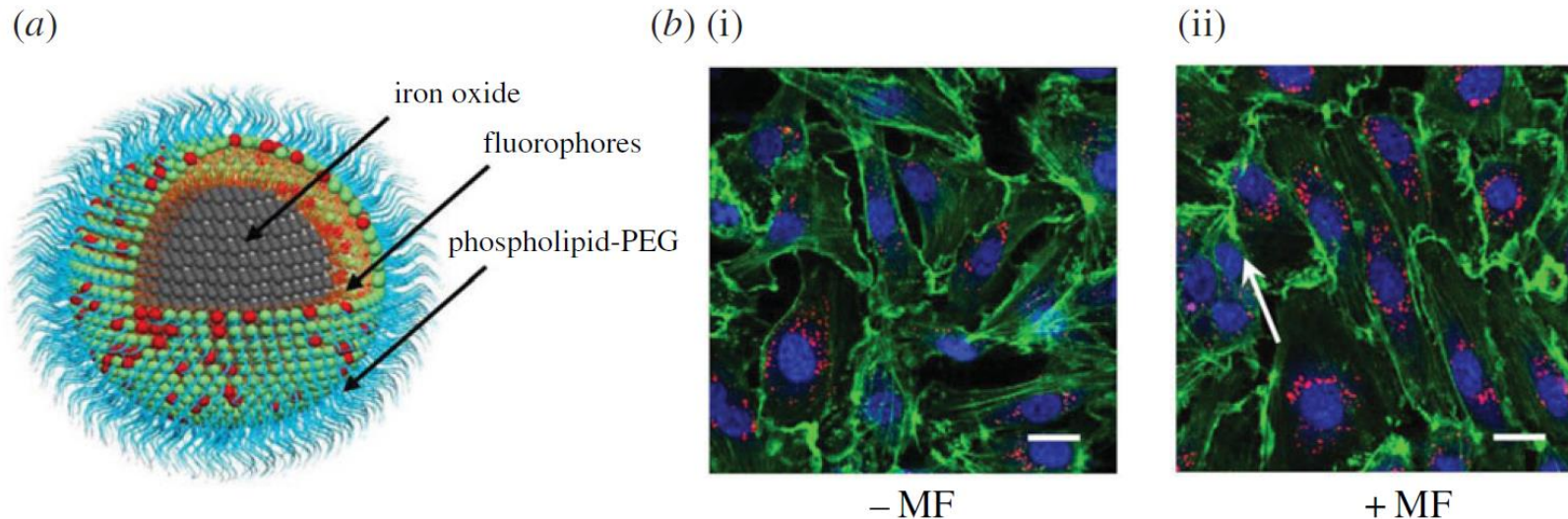
Interplay effect: interpretation



- Anomalous vascular dynamics of nanoworms within blood Flow
- Adhesion effect on margination of elastic micro-particles
- **Motion of particle under external magnetic field**
Active targeting: External triggering

Magnetic Guidance of Particle Penetration through Leaky Wall





Experimental results for enhanced permeability of vascular endothelium by an external magnetic field. (a) Schematic diagram of magnetic particle containing a magnetite nanocrystal and a phospholipid-polyethylene glycol (PEG) coating. (b) Endothelial cells containing magnetic particles incubated without and with magnetic field. (c) Particles with magnetism were injected into a mouse lateral tail vein, and the opposite lateral tail vein was placed under the external magnetic field. (d) Magnetic particles in the mouse tails quantified by a superconducting quantum interference device. Qiu *et al.* 2017 *Nat. Commun.* 8, 15594.

Conclusion:

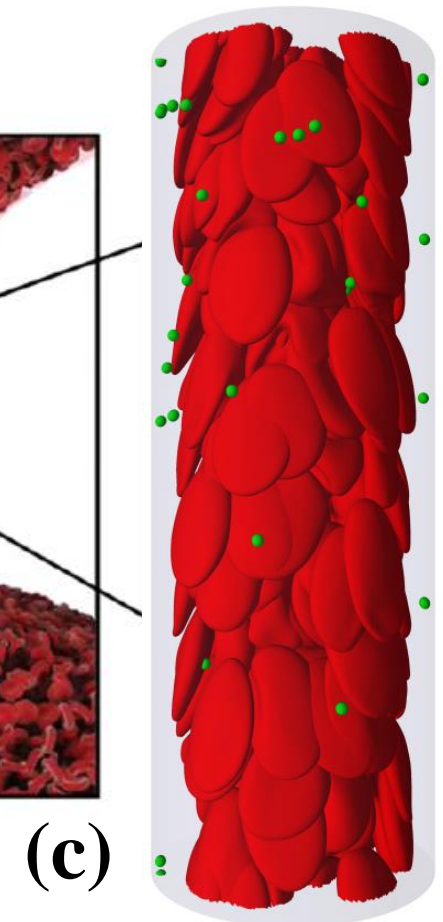
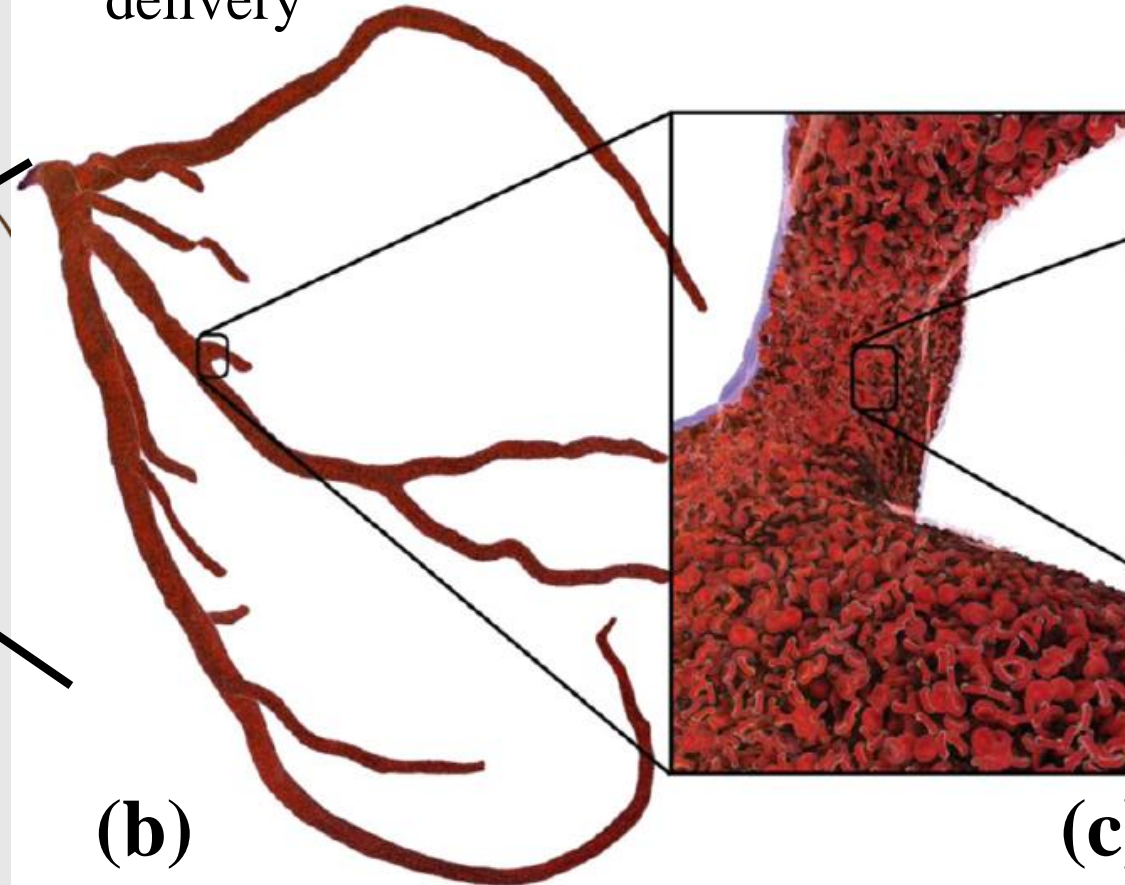
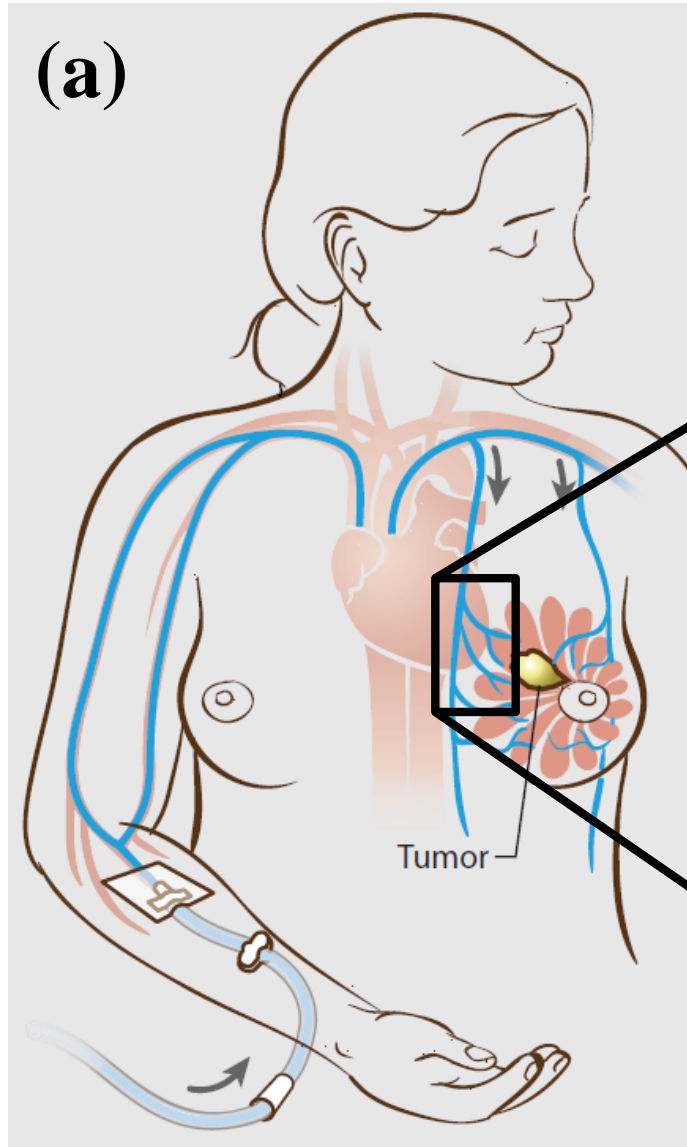
- ❑ Filamentous nanoworms can circulate longer than spherical particle in blood flow
- ❑ Margination of elastic particles: softer is not always better
- ❑ External triggering magnetic field can guide the accumulation of particle at near wall and promote the permeation through leaky wall

Ongoing work:

- ❑ Lattice Boltzmann method → complex vascular network modeling with machine learning technique (Graph Neural Network, GNN)
- ❑ GPU-accelerated blood flow simulations (multi-platform HPCs)

Anticipated outcome

- Advanced cyberinfrastructure for modeling NP transport
- Nanomedicine design tool
- High impact on diagnostic imaging and targeted drug delivery



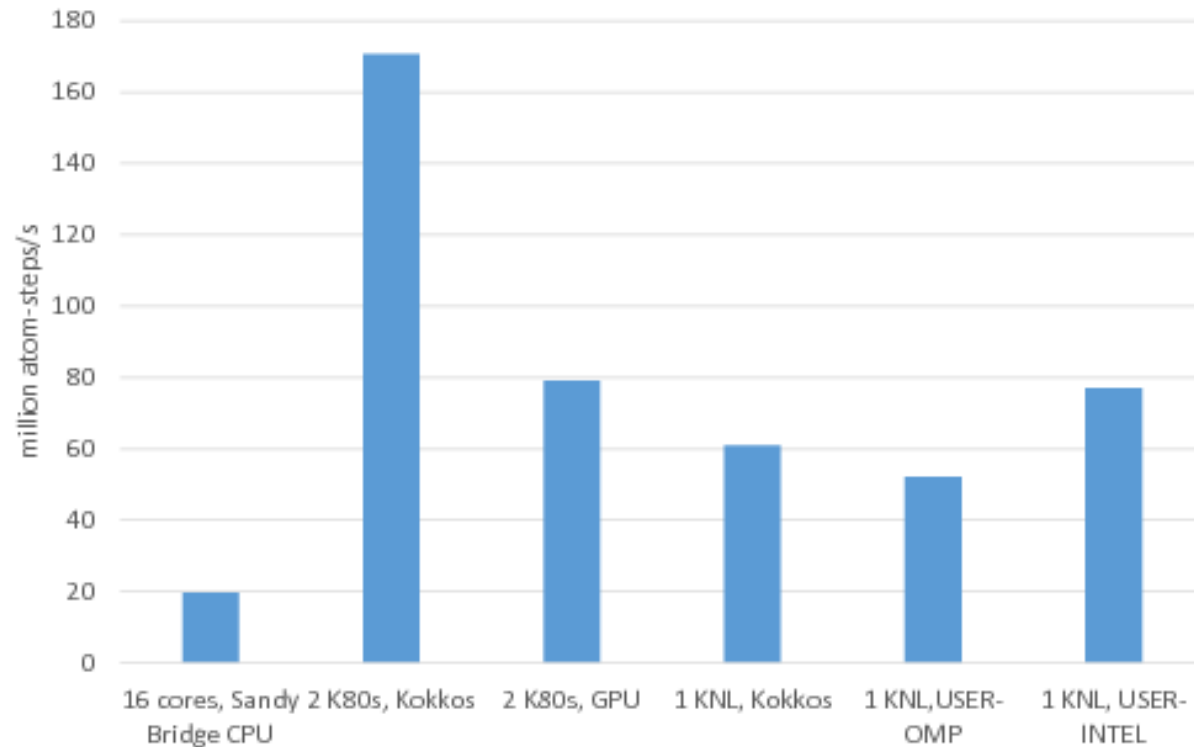
Goals: Portable, Performant, and Usable (<https://github.com/kokkos>)

- ❑ **Portable to Advanced Manycore Architectures**
 - Multicore CPU, NVidia GPU, Intel Xeon Phi (potential: AMD Fusion)
 - Maximize amount of user (application/library) code that can be compiled without modification and run on these architectures
 - Minimize amount of architecture-specific knowledge that a user is required to have
 - Allow architecture-specific tuning to easily co-exist
 - Only require C++1998 standard compliant
- ❑ **Performant**
 - Portable user code performs as well as architecture-specific code
 - **Thread scalable – not just thread safety (no locking!)**
- ❑ **Usable**
 - Small, straight-forward application programmer interface (API)
 - **Constraint: don't compromise portability and performance**

Accelerator benchmarks for CPU, GPU, KNL for LAMMPS

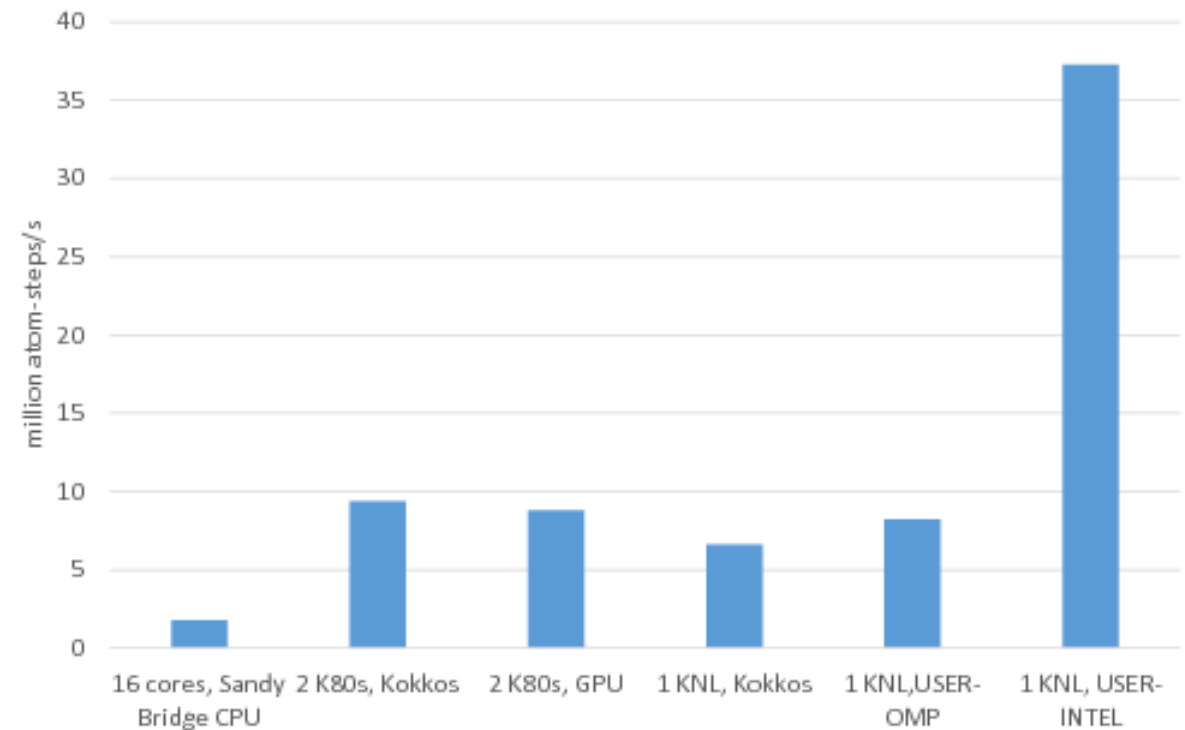
Benchmark of the Lennard-Jones potential

Lennard-Jones, 512K atoms



Benchmark of the Tersoff potential

Tersoff, 512K atoms



16 cores, Sandy Bridge CPU: no accelerator package, 1MPI task per core = 16 MPI tasks total

2 K80 GPUs, Kokkos: Kokkos package used 1 MPI task per internal K80 GPU = 4 MPI tasks total, running on 4 Sandy Bridge CPU cores, half neighbor list, newton on

2 K80 GPUs, GPU: GPU package used 4 MPI tasks per internal K80 GPU = 16 MPI tasks total, running on 16 Sandy Bridge CPU cores

1 KNL, Kokkos: Kokkos package used 64 MPI tasks x 4 hyperthreads x 4 OpenMP threads, half neighbor list, newton on

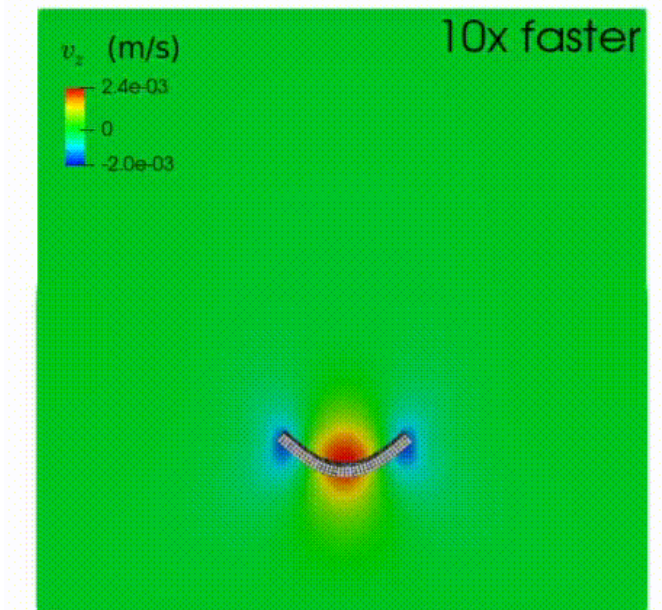
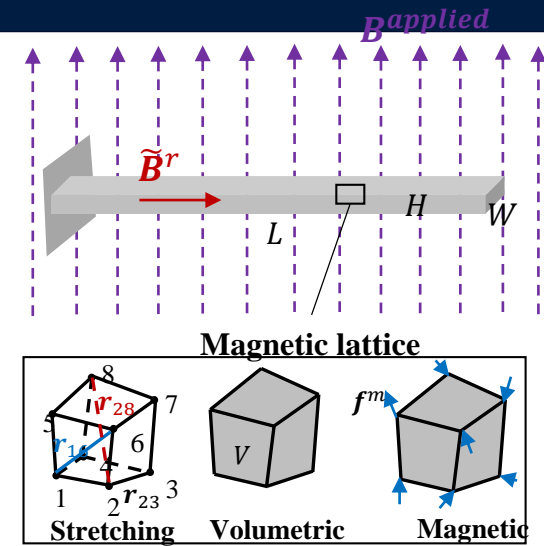
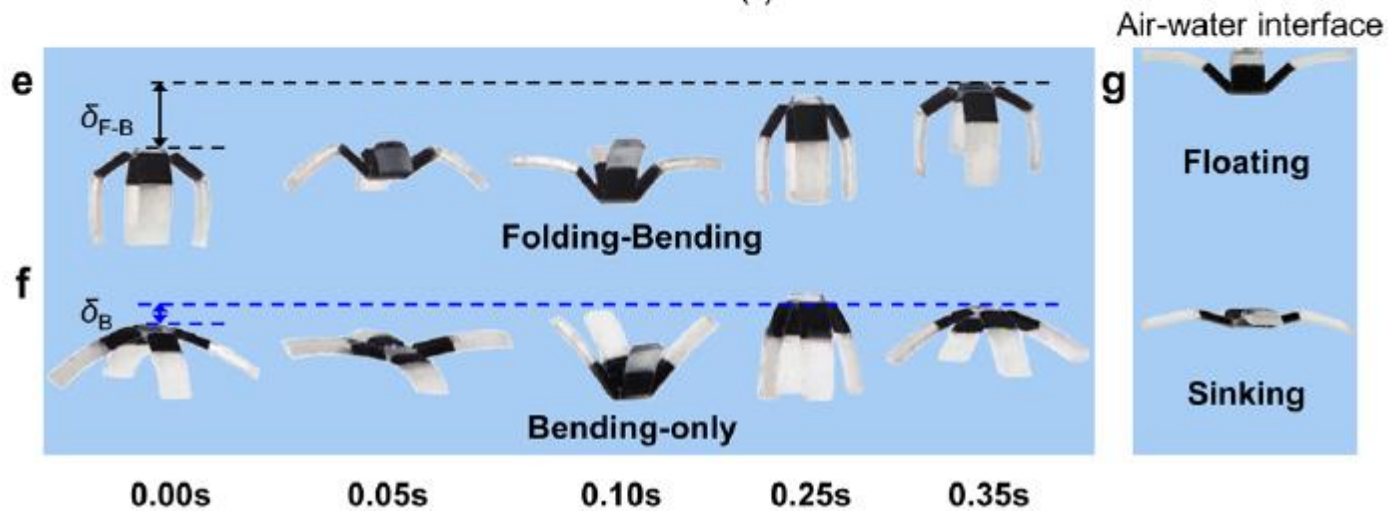
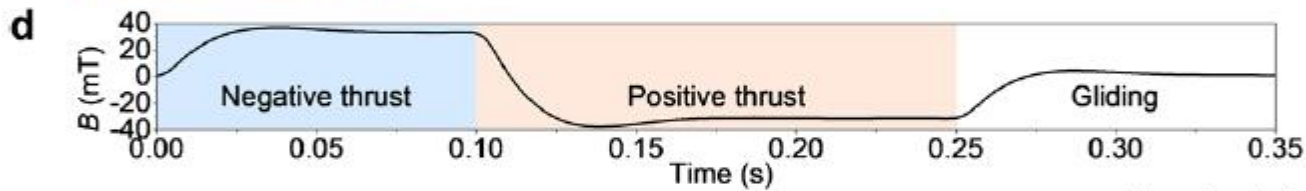
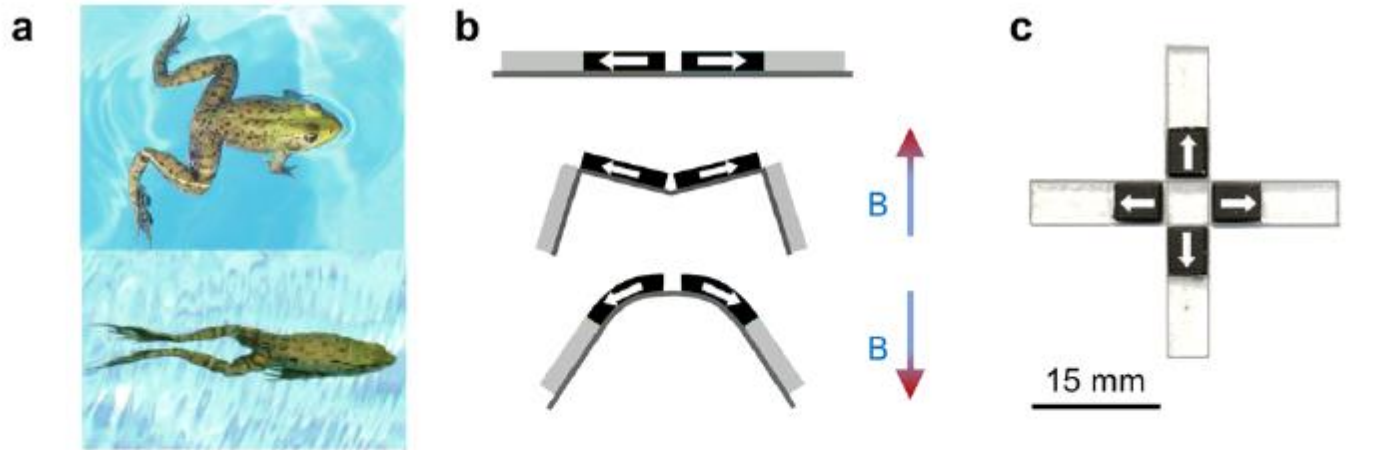
1 KNL, USER-OMP: USER-OMP package used 64 MPI tasks x 4 hyperthreads x 4 OpenMP threads

1 KNL, USER-INTEL: USER-INTEL package used 64 MPI tasks x 4 hyperthreads x 4 OpenMP threads

Future Work: magnetic soft robotic

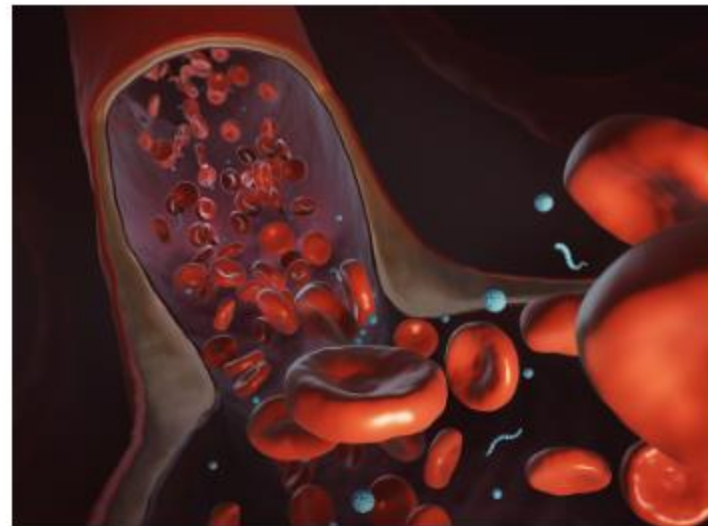
Manipulation of soft robotic under magnetic control

Wu, S. et al (2019) *ACS applied materials & interfaces*



- **Ye, H., Shen, Z., & Li, Y. (2021).** Adhesive rolling of nanoparticles in a lateral flow inspired from diagnostics of COVID-19. ***Extreme Mechanics Letters***, 44, 101239.
- **Ye, H., Shen, Z., Xian, W., Zhang, T., Tang, S., & Li, Y. (2020).** OpenFSI: A highly efficient and portable fluid–structure simulation package based on immersed-boundary method. ***Computer Physics Communications***, 256, 107463.
- **Ye, H., Shen, Z., Wei, M., & Li, Y. (2021).** Red blood cell hitchhiking enhances the accumulation of nano-and micro-particles in the constriction of a stenosed microvessel. ***Soft Matter***, 17(1), 40-56.
- **Ye, H., Shen, Z., & Li, Y. (2019).** Interplay of deformability and adhesion on margination of elastic micro-particles in blood flow. ***Journal of Fluid Mechanics***
- **Ye, H., Shen, Z., & Li, Y. (2018).** Shape dependent transport of micro-particles in blood flow: from margination to adhesion. ***Journal of Engineering Mechanics (Best Paper Selected by EMI FDTC)***
- **Ye, H., Shen, Z., Yu, L., Wei, M., & Li, Y. (2018).** Manipulating nanoparticle transport within blood flow through external forces: an exemplar of mechanics in nanomedicine. ***Proc. R. Soc. A***, 474(2211), 20170845
- **Ye, H., Shen, Z., & Li, Y. (2017).** Cell Stiffness Governs its Adhesion Dynamics on Substrate under Shear Flow. ***IEEE Transactions on Nanotechnology***
- **Ye, H., Shen, Z., & Li, Y. (2017).** Computational Modeling of Magnetic Particle Margination within Blood Flow through LAMMPS. ***Computational Mechanics*** (2017): 1-20.
- **Ye, H., Shen, Z., Yu, L., Wei, M., & Li, Y. (2017).** Anomalous Vascular Dynamics of Nanoworms within Blood Flow. ***ACS Biomater. Sci. Eng.***

Thank You!



TARGETING TUMORS WITH NANOWORMS

Published on April 28, 2021 by Aaron Dubrow

University of Connecticut engineer uses supercomputers and AI to improve delivery of nanomedicines for cancer

<https://www.tacc.utexas.edu/-/targeting-tumors-with-nanoworms>